2010-01-01

Reactive Oxygen Species Induced Cytokine Production and Cytotoxicity of PAMAM Dendrimers in J774a.1 Cells

Pratap Naha
Technological University Dublin, pratap.naha@tudublin.ie

Maria Davoren
Technological University Dublin, Maria.davoren@tudublin.ie

Fiona Lyng
Technological University Dublin, fiona.lyng@tudublin.ie

See next page for additional authors

Recommended Citation

Naha, P. et al (2010) Reactive Oxygen Species Induced Cytokine Production and Cytotoxicity of PAMAM Dendrimers in J774a.1 Cells. *Toxicology and Applied Pharmacology,* Vol.246, issue 1-1,pp.91-99. doi:10.1016/j.taap.2010.04.014

Funder: The INSPIRE programme, funded by the Irish Government's Programme for Research in Third Level Institutions, Cycle 4, National Development Plan 2007-2013, supported by the European Union Structural Fund.

Reactive Oxygen Species induced cytokine production and cytotoxicity of PAMAM dendrimers in J774A.1 cells.

Pratap C. Naha[a,b]*, Maria Davoren[a], Fiona M. Lyng[a] and Hugh J. Byrne[b]

[a]Radiation and Environmental Science Centre, Focas Research Institute, Dublin Institute of Technology, Kevin Street, Dublin 8, Ireland.

[b]NanoLab, Focas Research Institute, Dublin Institute of Technology, Kevin Street, Dublin 8, Ireland.

***Corresponding Author**

Pratap C. Naha,

Radiation and environmental Science Centre

Focas Research Institute, Dublin Institute of Technology,

Kevin Street, Dublin 8, Ireland.

E mail address: pratap.naha@dit.ie

Ph: +353 1 4027956

Fax : +353 1 402 7901

Abstract

The immunotoxicity of three generation of polyamidoamine (PAMAM) dendrimers (G-4, G-5 and G-6) was evaluated in mouse macrophage cells *in vitro*. Using the Alamar blue and MTT assays, a generation dependent cytotoxicity of the PAMAM dendrimers was found whereby G-6> G-5> G-4. The toxic response of the PAMAM dendrimers correlated well with the number of surface primary amino groups, with increasing number resulting in an increase in toxic response. An assessment of intracellular ROS generation by the PAMAM dendrimers was performed by measuring the increased fluorescence as a result of intracellular oxidation of Carboxy H_2DCFDA to DCF using a plate reader as well as by confocal laser scanning microscopy. The inflammatory mediators Macrophage Inflammatory Protein-2 (MIP-2), Tumour Necrosis Factor -α (TNF-α) and Interleukin -6, (IL-6) were measured by the enzyme linked immunosorbant assay (ELISA) following exposure of mouse macrophage cells to PAMAM dendrimers. A generation dependent ROS and cytokine production was found, which correlated well with the cytotoxicological response and therefore number of surface amino groups. A clear time sequence of increased ROS generation (maximum at ~4hrs), TNF-α and IL-6 secretion (maximum at ~24hrs), MIP-2 levels and cell death (~72 hrs) was observed. The intracellular ROS generation and cytokine production induced cytotoxicity point towards the mechanistic pathway of cell death upon exposure to PAMAM dendrimers.

Key words : Nanotoxicology, PAMAM dendrimers, Reactive Oxygen Species, cytokine production, macrophage, *in vitro.*

Introduction

Dendrimers have a well-defined nanoscale architecture and potential novel applications in the biomedical field (Lee et al., 2005). Polyamidoamine (PAMAM) dendrimers contain a 2-carbon ethylenediamine core and primary amino groups on the surface (http://www.dendritech.com/pamam.html.). The systematically variable structural architecture and the large internal free volume make these dendrimers an attractive option for drug delivery and other biomedical applications (Venuganti and Perumal 2008; Svenson and Tamalia 2005; Emanuele and Attwood 2005; Ducan and Izoo 2005). It is possible to passively target PAMAM dendrimers to a tumour because of the increased permeability of tumour vasculature to macromolecules and also due to the limited lymphatic drainage (Maeda and Matsumura 1986). The unique properties of dendrimers, as compared to linear polymers, render them of interest for intracellular drug delivery system for cancer therapy (Gillis and Frechet 2005). PAMAM dendrimers have been utilised for gene delivery (Yoo and juliano 2000; Huang et al., 2007) and also as delivery agents for antisense and siRNA oligonucleotides (Kang et al., 2005). Dendrimers have been considered as additives in several routes of administration, including intravenous, oral and ocular (Cheng et al., 2008). Amino terminated PAMAM dendrimers result in enhanced anti-ovalbumin immunoglobulin-G and immunoglobulin-M levels and have also been used as adjuvants in vaccine delivery systems (Rajananthanan et al., 1999). In a recent study it has been shown that N-acetyl-D-glucosamine modified PAMAM dendrimers improve the immunogenicity by up-regulation of antibody formation via activation of natural killer cells (Hulikova et al., 2009) and the mannosylated form of PAMAM dendrimers potentiate the immunogenicity and have been proposed for vaccine delivery systems (Sheng et al., 2008).

The application of nanomaterials as intravenous drug delivery platforms may depend on avoiding rapid elimination from the systemic circulation by cells of the immune system. When nanoparticles enter into the bloodstream, they immediately encounter a complex environment of plasma proteins and immune cells. The interaction of nanoparticles with immune cells may occur both in the blood stream via monocytes, platelets, leukocytes, and dendritic cells (DC) and in tissues by resident phagocytes, e.g., Kupffer cells in liver, DC in lymph nodes, macrophages and B cells in the spleen (Dobrovolskaia et al., 2008). As PAMAM dendrimers are potentially proposed for vaccine and intracellular gene delivery applications, and macrophages are the main target cells to produce/improve the immunogenicity of the different antigens, this study explores the understanding of the

interaction with and toxicity to macrophages cells of PAMAM (G-4, G-5 and G-6) dendrimers. J774A.1 cells, derived from the blood of female BALB/c mouse, are chosen for the in vitro model. ROS and subsequent cytokine production are monitored as indicators of oxidative stress and inflammatory response.

In addition to a study of the PAMAM dendrimer materials in their own right, the systematically varied molecular nanostructures potentially provides a route towards an understanding of the dependence of the interactions on the physico-chemical properties of nanomaterials. In a recent study, the toxicity of PAMAM dendrimers in mammalian cells has been demonstrated to be generation dependent (Mukherjee et al., 2009), potentially laying the foundation for structure-activity relationships underlining the mechanistic responses. Conjugation of poly (ethylene glycol) (PEG) to the surface of PAMAM dendrimers has been observed to improve their biocompatibility, reducing the cytotoxic response (Wang et al., 2009). Nanoparticle toxicity has been proposed to have origin in the induction of oxidative stress by free radical formation (Nel et al., 2006; Lanone et al., 2006; Donaldson et al., 2006; Obedoster et al., 2005). In excess, free radical formation causes damage to biological components through oxidation of lipids, proteins and DNA. Oxidative stress may have a role in the induction of inflammation through up regulation of redox sensitive transcription factors, NF-κB and activator protein-1 (AP-1), and kinases involved in inflammation (Lanone et al., 2006; Rahman, 2000; Rahman et al., 2005; Park and Park 2009).

The objective of the present work is an *in vitro* assessment of the immunotoxicological response of three generations of the cationic PAMAM dendrimers (G-4, G-4 and G-6) in mouse macrophage cells (J774A1). The systematically varied structure and size allows an evaluation of the dependence of the response on the physico–chemical properties. The PAMAM dendrimers were characterized in terms of particle size and zeta potential in cell culture media with and without protein (FBS). In accordance with the EU policy of Reduction, Replacement and Refinement (RRR) an *in vitro* rather than animal model is employed to assess the cytotoxic response and underlying mechanisms of these materials. (Directive 86/609/EEC on the protection of animals used for experimental and scientific purposes). Cytotoxicological effects of PAMAM dendrimers were evaluated using the Alamar blue and MTT [(3-(4, 5-Dimethylthiazol-2-yl)-2, 5- diphenyltetrazolium bromide, a tetrazole)] assays. Intracellular reactive oxygen species (ROS) were measured following exposure of the macrophages to PAMAM dendrimers for time periods of 1h, 2h, 4h and 6h. The visualisation of ROS production by the cells was performed by confocal laser scanning

microscopy. The secretion of the cytokines and chemokines, Macrophage Inflammatory Protein-2 (MIP-2), Tumour Necrosis Factor -α (TNF-α) and Interleukin -6 (IL-6), following exposure of the macrophage cells to PAMAM dendrimers was measured quantitatively by enzyme linked immunosorbant assay (ELISA).

MATERIALS AND METHODS

Test materials

Polyamidoamine (PAMAM) dendrimers, G4, G5 and G6, were purchased from Sigma Aldrich Ltd. (Dublin, Ireland). All the particles have an ethylenediamine core and PAMAM G4, G5 and G6 have respectively 64, 128 and 256 functional primary amino groups on the surface. The molecular weights of G4, G5 and G6 are 14,215 Da, 28,826 Da and 58,048 Da respectively. The nominal diameters of the G4, G5 and G6 dendrimers are 4.5, 5.4 and 6.7 nm respectively [Dendritech, Sigma Aldrich Ltd., (Supporting information, Table S1)]. The diameter and zeta potential of the dendrimers were measured using a Malvern Zeta Sizer Nano ZS (Malvern Instruments, Worcestershire, UK). The measurements were performed on 20μM dendrimer solutions in J774A1 cell culture media at 24°C and compared to those in MilliQ water and DMEM cell culture medium, shown in table S2.

Reagents

3-(4,5-dimethylthiazol-2-yl)-2,5-diphenyltetrazolium bromide (MTT), and 2,2'-Azino-Bis(3-Ethylbenzthiazolin-6-Sulfonic acid), were purchased from Sigma Aldrich Ltd. (Dublin, Ireland). Alamar Blue (AB) was purchased from Biosource (UK). Cell culture media (DMEM, D5546) and supplements were purchased from Sigma Aldrich Ltd. (Dublin, Ireland) and Bioscience (Dublin, Ireland). 5-(and 6) Carboxy-2', 7'-dichloro-dihydroflourescein diacetate (H_2DCFDA, Invitrogen, 522406), IL-6 (900-K50), MIP-2 (900-K152), TNF-α (900-K52) ELISA kits were purchased from Peprotech (UK).

Cell Culture

J774A.1 is a mouse macrophage cell line, (ECACC, 91051511) derived from tumour in a female BALB/c mouse. J774A.1 cells were cultured in Dublecco's Modified Eagle's Medium (DMEM) with 2mM L-glutamine supplemented with 10% fetal bovine serum (FBS), 45 IU ml^{-1} penicillin and 45 IU ml^{-1} streptomycin at 37ºC in 5% CO_2 .

Preparation of Dendrimer solution

Dendrimer test solutions were prepared in the cell culture media, under laminar flow and sterile conditions. They were soluble in the media at 37 ºC and were dispersed uniformly by low speed vortex. The concentration ranges used for the cytotoxicity assays with G4, G5 and G6 were 0.08 μM to 6 μM; 0.03 μM to 2 μM; and 0.013 μM to 1 μM respectively, as determined from an initial range finding study.

Throughout this study, molar concentrations have been chosen as the unit of preference as they enable the response to be easily conceptualised in terms of number of particles, surface area and/or number of surface groups. For comparison, 1M – xxxxg/l for G4, yyy g/l for G5 and zzzg/l for G6, respectively.

Cytotoxicity assays

Alamar blue (AB) and MTT assays were employed to assess the cytotoxicity of PAMAM dendrimers with the mouse macrophages (J774A.1) cells.

Alamar blue (AB) assay

For the cytotoxicity test, wells are plated with 100 μl of the following cell suspension concentration: 1×10^5 cells/ml for 6, 12, and 24 h exposure; 8×10^4 cells/ml for 48 h exposure and 6×10^4 cells/ml for 72 h exposure in 96-well microplates (Nunc, Denmark). After 24h of cell attachment, plates were washed with 100 μl/well PBS and the cells were treated with increasing concentrations of each generation of dendrimer prepared in 5% FBS containing media. All incubations were performed at 37°C in a 5% CO_2 humidified incubator. Six replicate wells were used for each control and test concentrations per microplate.

The assays were carried out according to the manufacturer's instruction. Briefly, control media or test exposures were removed; the cells were rinsed with PBS and 100μl of AB medium (5% v/v solution of AB) prepared in fresh media (without FBS or supplements) were added to each well. After 3h incubation, AB fluorescence was measured at the respective excitation and emission wavelength of 540 nm and 595 nm in a microplate reader (TECAN GENios, Grodig, Austria).

MTT assay

A parallel set of plates was set up for the MTT assay and seeded and exposed in an identical manner to that described in AB assay. After 24h of PAMAM dendrimer exposure, the control medium or test exposures was removed, the cells were washed with PBS and 100 µl of freshly prepared MTT in media (5 mg/ml of MTT in un-supplemented media) were added to each well. After 3h incubation, the medium was discarded and the cells were rinsed with PBS and 100 µl of DMSO were added to each well to extract the dye. The plates were shaken at 240 rpm for 10 min and the absorbance was measured at 595 nm in a microplate reader (TECAN GENios, Grodig, Austria).

Intracellular Reactive Oxygen Species (ROS)

Intracellular reactive oxygen species were measured by a fluorimetric assay using Carboxy H_2DCFDA as the probe. Carboxy H_2DCFDA was used because it carries an additional negative charge that improves its retention compared to non-carboxylated forms (http://probes.invitrogen.com/media/pis/g002.pdf). Intracellular oxidation of Caroxy H_2DCFDA to DCF was monitored according to the increase in fluorescence as measured by a plate reader and using confocal fluorescence microscopy. In brief, the assay was performed in black 96 well microplates (Nunc, Denmark). The J774A.1 cells were seeded in 100 µl of cell suspension in each well at a density of 4 x 10^5 cells/ml. After 24 h of cell attachment, plates were washed with 100 µl/well PBS and the cells were treated with increasing concentrations of each generation of dendrimer prepared in 5% FBS containing media. Hydrogen peroxide (400 µM) was used as positive control to validate the protocol. All incubations were performed at 37°C in a 5% CO_2 humidified incubator. Six replicate wells were used for each control and test concentrations per 96 well microplate. After the specified incubation time period (1, 2, 4 and 6 h) the plates were washed with 100 µl/well PBS and then 100 µl/well of 10 µM Carboxy H_2DCFDA was added to each well. The plates were incubated at 37°C for a period of 40 minutes. The fluorescence was quantified using a plate reader, which provides an average of the statistically variable response of individual cells (Elbekai and El-Kadi, 2005). Fluorescence was measured using an excitation of 485 nm and emission of 530nm, in a TECAN GENios (Grodig, Austria) microplate reader. For visualisation of the intracellular fluorescence, carboxy H_2DCFDA was excited at 488 nm and fluorescence emission at 520 nm (with a 505 nm long pass filter) was recorded using a confocal laser scanning microscope (LSM 510 META, Zeiss, Germany). Fluorescence and phase contrast images were recorded from a minimum of 3 areas per sample.

Cytokines assay

An enzyme linked immunosorbant assay (ELISA) was performed to quantify the proinflammatory mediators (IL-6, TNF-α and MIP-2) after the exposure of the J774A.1 cells to PAMAM dendrimers. The low cost, routine technique is widely used to monitor and quantify the production of cytokines and is favoured over the relatively time consuming and costly techniques of qRT PCR (*Osuchowski et al., 2005, 2006, Batista Jr. et al. 2006)*. LPS (lipo-polysaccharide) was used as positive control to stimulate the TNF-α and MIP-2 and validate the ELISA protocol. The principle of the ELISA is based on the sandwich technique, in which the capture antibody (primary antibody) at concentrations of 1μg/ml (TNF-α), 2 μg/ml (IL-6) and 0.5 μg/ml (MIP-2) in PBS (pH -7.4) , was coated in the 96 well plate (Nunc-immuno plate, Denmark). The plates were incubated over night at room temperature. The wells were aspirated to remove the liquid and the plates were washed four times with PBS-T (phosphate buffer saline with 0.05% of Tween 20) and then blocked with 1% BSA solution at room temperature for 1 hour. The plates were again washed with PBS-T four times and 100 μl of different dilutions of supernatant were added to the respective wells and standards of IL-6, TNF-α and MIP-2 at a concentration from 10 to 800 pg/ml in duplicate were added to the first two columns of the 96 well plates and incubated for 2h at room temperature. The plates were aspirated and washed four times, whereupon 100μl of the detection antibody against the respective marker (secondary antibody) were added to the 96 well ELISA plate at a concentration of 0.25μg/ml (for TNF-α and MIP-2), or 0.5 μg/ml (IL-6) and the plates were incubated at room temperature for 2h. The plates were aspirated and washed four times, 100 μl of avidine-HRP (1:2000 dilutions in blocking buffer) were added to each well and the plates were incubated for 30 minutes at room temperature. The plates were washed four times with washing buffer and 100 μl of substrate solution (2,2'-Azino-Bis(3-Ethylbenzthiazolin-6-Sulfonic acid)) were added to each well and the plates were incubated at room temperature to develop the colour. The colour development time was optimised to be 15 minutes for each assay using the standards and the absorbance was measured at 405 nm in a VICTOR^{3}V^{TM} 1420 Multilabel Counter plate reader (Perkin Elmer, USA).

Statistics

All experiments were conducted in at least triplicate (three independent experiments). Fluorescence as fluorescent units (FUs) of all of the assays was quantified using a microplate reader (TECAN GENios, Grödig, Austria). Raw data from cell cytotoxicity assays, all the ELISA and ROS data were collected and analyzed using Microsoft Excel® (Microsoft Corporation, Redmond, WA). Cytotoxicity and ROS data were expressed as mean percentage viability relative to the unexposed control (100%) ± standard deviation (SD). MIP-2, IL-6 and TNF-α data were calculated from their respective standards and were expressed in mean (pg/ml) ± standard deviation (SD). Statistical analyses were carried out using one-way analyses of variance (ANOVA) followed by Dunnett's multiple comparison tests. Statistical significance was accepted at $P \leq 0.05$ for all tests. Toxicity data was fitted to a sigmoidal curve and a four parameter logistic model was used to calculate EC_{50} values. This analysis was performed using Xlfit3™ a curve fitting add-in for Microsoft® Excel (ID Business Solutions, UK).

RESULTS

Characterisation of PAMAM dendrimers

The PAMAM dendrimers (G-4, G-5 and G-6) were characterised in terms of particle size, and zeta potential. From our previous study, the hydrodynamic diameter correlated well with that quoted by the manufactures (Naha et al., 2009). In the J774A.1 cell culture media, the hydrodynamic diameter of G-4, G-5 and G-6 was 6.2 nm ± 0.3 nm; 7.5 nm ± 0.3 nm and 10.3 nm ± 0.4 nm respectively. The slight increase in size in cell culture media may be due to the interaction with proteins or other components of the cell culture media producing a 'protein corona' as has been observed with other nanoparticles (Lynch et al., 2007).

In Milli Q water and DMEM cell culture medium, the zeta potential of the PAMAM dendrimers was observed to be positive, due to the cationic surface amino group. However, the surface charge was observed to be negative in the J774A1 cell culture medium containing 5% FBS due to the interaction of proteins with the surface amino group, as observed in our previous study (Naha et al., 2009). The zeta potential of G-4, G-5 and G-6 was found to be -2.9 ± 1.1; -3.1 ± 0.9; and -3.9 ± 0.4 mV respectively (Table 1)**.** This is a clear indication of the interaction of the protein with the PAMAM dendrimers as shown previously (Naha et al., 2009).

Cytotoxicity assay

The cytotoxicity of PAMAM dendrimers was determined using two different assays for an exposure time of 24h and the results are shown in Figure 1, with the EC_{50} values shown in Table 2. The toxic response observed in both assays is well matched and there is no significant difference between the calculated EC_{50} from both the assays in J774A1 cells.

A time and generation dependent toxic response was furthermore observed as shown in Figure 2a. Maximum cell death occurs at 72 h exposure of all the three generation of PAMAM dendrimers. The trend of toxic response was G-6 > G-5 > G-4, as observed previously for aquatic species and fish cell lines (Naha et al., 2009) as well as mammalian cell lines (Mukherjee et al., 2009). Notably, the toxic response in terms of inverse EC_{50} (Ragnvaldsson et al., 2007) is linearly correlated with the number of surface primary amino group present in the PAMAM dendrimers shown in Figure 2.b for the case of 24 h exposure, demonstrating a clear structure-activity relationship. In order to further explore the mechanisms of cell death, the induced oxidative stress and inflammatory response were explored.

Intracellular Reactive oxygen species (ROS)

The intracellular ROS study was performed at different time points (1, 2, 4 and 6h) and with different exposure concentrations of each dendrimers (G-4, G-5 and G-6). For all generations, the exposure time points and the concentration of PAMAM dendrimer (0.031 μM to 3 μM) used were the same, in order to correlate the increased ROS production by the three generations of PAMAM dendrimers and also to enable comparison with the cytotoxic and inflammatory response. Intracellular ROS production in the macrophage cells upon the exposure to PAMAM dendrimers was easily visualised using confocal fluorescence microscopy, as shown in figure 3 for the case of 2 h exposure of each dendrimer at a concentration of 1 μM. The fluorescence was quantified using a plate reader, which provides an average of the statistically variable response of individual cells (Elbekai and El-Kadi, 2005). This in situ method was favoured over flow cytometry as J7741.A cells are strongly adherent and do not detach easily from the flask after trypsinisation. The concentration dependent increase in ROS production for four different time points for the three dendrimer generations was monitored and the results are shown in the supporting information (Figure S1a-d). Increased ROS production was found to be dendrimer generation and time dependent (Figure 4a). In a previous study of poly (propyleneimine) dendrimers (PPI), a similar generation dependent intracellular ROS production and reduction of mitochondrial membrane

potential was observed in macrophages (Kuo et al., 2007). The generation dependence follows the trend of G-6 > G-5 > G-4, as was seen for the cytotoxic response. Similar to the case of the cytotoxic response, the generation dependent ROS levels appear to be correlated with the increase of surface primary amino group with increasing generation, as shown in figure 4b for the case of 1 h exposure.

Cytokines production

Macrophage inflammatory protein-2 (MIP-2)

The level of macrophage inflammatory protein-2 (MIP-2) secretion by the J774A.1 cells following exposure to PAMAM dendrimers was analysed from the cell culture supernatant after exposure to 5 different concentrations of each dendrimer and also at 5 different exposure time periods (6, 12, 24, 48 and 72h). MIP-2 levels at different exposure time periods were calculated from the standard curve of the MIP-2 standards (ranging from 10 to 800 pg/ml). The secretion of MIP-2 level was found to be time, PAMAM generation and concentration dependent, as shown in Figures 5a-c and 6. Maximum levels of MIP-2 were generated at all the time points at concentrations of G-4 (1.2 μM); G-5 (0.4μM) and G-6 (0.2 μM) and The secretion of MIP-2 protein from the macrophage cell was found to be generation dependent, G-6 producing the highest level and G-4 the lowest, (G-6 > G-5 > G-4) which is well correlated with the cytotoxic response and the ROS generation. Although a linear dependence is not obvious, the MIP-2 protein secretion levels increase monotonically with the number of surface primary amino group of the PAMAM dendrimer, as shown in Figure 7a.

Interleukin-6 (IL-6)

The levels of IL-6 in after different exposure time periods (6, 12, 24, and 48 h) were calculated from the standard curve of IL-6 standards (ranging from 10 to 800 pg/ml). In the case of G-4 (0.6 μM); G-5 (0.4 μM) and G-6 (0.2 μM), the maximum levels of IL-6 were observed after 24 h exposure. A generation dependent IL-6 secretion from the macrophage cells was observed upon the exposure to PAMAM dendrimers as shown in Figure 6, G-6 producing the highest levels and G-4 the lowest (G-6 > G-5 > G-4) which is well correlated with the cytotoxic response. Again the level of IL-6 secretion by the J774A.1 cells increases monotonically with the surface area of the each dendrimer generation, as shown in Figure 7 b. The secretion of IL-6 was time dependent, generation dependent and concentration of PAMAM dependent shown in supporting information (Figure S2a-c).

Tumour necrosis factor-α (TNF-α)

The TNF-α levels at different exposure times (6, 12, 24, and 48 h) were calculated from the standard curve of TNF-α standards (ranging from 10 to 800 pg/ml). Maximum levels of TNF-α were generated at concentrations of G-4 (1.2 μM); G-5 (0.8μM) and G-6 (0.2 μM) after 24h exposure. A generation dependent TNF-α secretion from the macrophage cells was observed upon the exposure to the dendrimers, G-6 producing the highest levels and G-4 the lowest, (G-6 > G-5 > G-4) (Figure 6) which is well correlated with the cytotoxic response. Again the levels of TNF-α secretion by the J774A.1 cells increase monotonically with the number of surface primary amino group of the PAMAM dendrimer, shown in Figure 7c. The secretion of TNF-α was found to be time dependent, PAMAM generation and concentration dependent shown in supporting information (Figure S3a-c).

DISCUSSION

The cytotoxic response of J774A.1 cells to the PAMAM dendrimers, with varying numbers of $–NH_2$ surface group (G-4, G-5 and G-6), was evaluated using the Alamar blue (AB) and MTT assays. The EC_{50} was calculated and no significant difference was observed between the assays after 24 h exposure (Figure 1). Alamar blue is a water-soluble dye and the oxidized form enters the cytosol and is converted to the reduced form by mitochondrial enzyme activity by accepting electrons from NADPH, FADH, FMNH, NADH as well as from the cytochromes (Al-Nasiry et al., 2007). Mitochondrial activity was determined by the MTT assay. MTT is reduced to the purple formazan in the mitochondria of living cells. This reduction takes place only when mitochondrial reductase enzymes are active, and therefore conversion can be directly related to the number of viable (living) cells. MTT is completely reduced by mitochondrial enzyme. The close agreement of the EC_{50} as determined by the two assays is an indication of significant mitochondrial injury as origin of the cytotoxic response.

The toxic response was seen to increase with dendrimer generation and therefore size. A similar generation dependent toxicological response was previously seen with fish cells (Naha et al., 2009) and also mammalian cells lines (Mukherjee et al., 2009). A toxic response

which increases with nanoparticle diameter would appear to go against the commonly accepted trends of increased toxicity with decreased nanoparticle size, but can be understood in terms of the linear correlation with the number of surface amino groups of PAMAM dendrimer as shown in Figure 2 b.

The surface primary amino groups render the dendrimers cationic and as the generation of PAMAM dendrimer increases, there is a linear increase in the number of surface amino groups (Dendritech, Inc. http://www.dendritech.com/pamam.html). The observed generation dependence suggests that the toxic response has origin in the actions of the surface charge (Figure 2b). Cationic particles have been shown to localise in mitochondria and produce a cytotoxic response via the mitochondrial injury pathway (Xia et al 2008 and 2006), generating ROS as a result (Nel et al., 2006; Lee et al., 2003).

In this study, intracellular ROS generation by PAMAM dendrimers is clearly one of the toxic pathways and a clear generation dependence of intracellular increased ROS production is shown in Figure 4a. The sequence of increased ROS generation is G-6> G-5 > G-4. This response is also well correlated with the number of surface primary amino group of PAMAM dendrimers, as shown in Figure 4b. This indicates that the cationic surface amino groups play a direct role in the production of ROS. Increased intracellular ROS generation suggests that the PAMAM dendrimers can lead to disruption of the mitochondrial electron transduction chain which leads to additional O_2^- production (Donaldson et al., 2005) and perturbs the mitochondrial permeability transition pore, which leads to release of pro-apoptotic factors and programmed cell death (Oberdorster et al., 2005).

Intracellular ROS production can lead to inflammation, as demonstrated for a number of different nanoparticles (Li et al., 2008; Stone et al., 2007; Lubos et al., 2008; Driscoll, 2000). Oxidative stress activates the MAPK signalling pathway, inducing transcription factors such as NFkB and AP-1, and these transcription factors induce mRNA expression of pro-inflammatory mediators and finally cause inflammation (Park and Park 2009). Macrophage inflammatory protein-2 (MIP-2) plays a major role in mediating the neutrophilic inflammatory response to nanoparticles (Driscoll et al., 1995). It is a potent neutrophil chemoattractant and epithelial cell mitogen and is involved in acute pulmonary inflammation and mediates tissue damage (Walley et al., 1997; Chung et al., 2003). It is induced by LPS (Lipopolysaccharide), oxidative stress in a wide range of cells including alveolar

macrophages, mast cells, peritoneal macrophages, epithelial cells and fibroblasts (Monteiller et al., 2007).

Inflammatory response induced by nanoparticles is thus a further toxic mechanism (Monteiller et al., 2007), and in this work we have highlighted the inflammatory mediators (MIP-2, TNF-α and IL-6) induced by PAMAM dendrimers. The level of secretion of all three inflammatory mediators, MIP-2, TNF-α and IL-6 following exposure of macrophage cells to PAMAM dendrimers is dependent on the concentration, time of exposure and the generation of PAMAM dendrimers, as well as the cytotoxic response. A generation dependent cytokine production was found in all cases and the trend was G-6 > G-5 > G-4. Thus the ROS production, inflammatory response and cytotoxicity all show similar trends in terms of dendrimer structure. The pathway of the toxic response induced by PAMAM dendrimers may therefore be one of localisation in the mitochondria (Lee et al., 2009) leading to disruption of the mitochondrial electron transduction chain, and additional O_2^- production (Donaldson et al., 2005) resulting in oxidative stress (Figure 3 and Figure 4) The systematic mechanistic pathways of cell death due to PAMAM dendrimers is presented in Figure 8a, and the sequence of responses as a function of time is shown in Figure 8b. Within the resolution of the measurements performed, the timing sequence is identical for all three dendrimer generations.

Although the toxic responses can be well correlated with the dendrimer generation structures, it should be noted that the particle size was seen to increase in the cell culture medium and furthermore that the zeta potential of the PAMAM dendrimers changed polarity from positive to negative. These observations point towards the interaction of proteins and/or other molecular components of the medium with the particle surface. In our previous study, we have seen spectroscopically the interaction of FBS with the PAMAM dendrimers (Naha et al., 2009), as has been documented for other nanoparticles, leading to the formation of a protein corona (Lynch et al., 2007). In the case of carbon nanotubes, such interactions have been shown to result in medium depletion and a secondary or indirect toxicity (Casey et al., 2008) even though the carbon nanotubes are not seen to be taken up by the cells (Davoren et al., 2007). From this point of view it is important to understand whether toxic responses originate from the interaction of particles external or internal to the cells.

Significant ROS generation has also been seen from carbon nanotubes external to the cells (Herzog et al., 2009). Thus it is conceivable that the ROS, cytokines production, cytotoxicity

cascade could be initiated from external stress (Herzog et al., 2009). However, a recent study has clearly demonstrated the internalisation of PAMAM dendrimers and their localisation in the mitocondria (Lee et al., 2009). Thus, although there may be external stress leading to some degree of indirect toxic response, it is proposed that the principal response is a direct result of internalisation of the nanomaterials.

CONCLUSIONS

PAMAM dendrimers show a significant cytotoxic response in mouse macrophage cells (J774A.1) *in vitro* at a concentration of 0.013 to 6 μM. The generation dependence (G-6 > G-5 > G-4) of the production of increased intracellular ROS, inflammatory mediators and the cytotoxicity indicates the direct effects of the positively charged surface amino groups. The mechanism of the toxic response is proposed to be one of localisation of the cationic particles in the mitochondria, leading to significant increase in ROS generation, induction of cytokines production and ultimately cell death. The generation dependent intracellular ROS levels, cytokines production and cytotoxicity of PAM AM dendrimers point towards the basis of structure activity relationships.

The choice of concentration ranges of the PAMAM dendrimer exposure for each study was guided by the manifestation of a generation dependent response. These concentrations are moreover of relevance for proposed therapeutic applications (Kukowska-Latallo et al., 2005). Based on the OECD Guidelines for acute oral toxicity (De Jong, 2009) and using an approximate guideline that *in vitro*, 1 mg/ml may be considered equivalent to 1g/kg (http://probes.invitrogen.com/media/pis/g002.pdf), the toxicity may be classified as the lowest Category, 5. As the toxicity may therefore be considered acceptable and based on the improvement in the cytokine production (TNF-α, MIP-2 and IL-6), PAMAM dendrimers may potentially be useful, for example as a vaccine delivering agent.

Acknowledgement : This work was conducted under the framework of the INSPIRE programme, funded by the Irish Government's Programme for Research in Third Level Institutions, Cycle 4, National Development Plan 2007-2013, supported by the European Union Structural Fund.

Reference

Al-Nasiry, S., Geusens, N., Hanssens, M., Luyte, C., and Pijnenborg R. 2007. The use of Alamar Blue assay for quantitative analysis of viability, migration and invasion of choriocarcinoma cells. Human Production 22, 1304-1309.

Casey, A., Herzog, E., Lyng, F. M., Byrne, H. J., Chambers, G., Davoren, M. 2008. Single walled carbon nanotubes induce indirect cytotoxicity by medium depletion in A549 lung cells. Toxico Lett. 179, 78–84.

Cheng, Y., Xu, Z., Ma, M., Xu, T. 2008. Dendrimers as drug carrier: applications in different routes of drug administration. J. Pharm. Sci. 97, 123-143.

Chung, Y-J., Yang, G H., Islam, Z., Pestka J. J. 2003. Up-regulation of macrophage inflammatory protein-2 and complement 3A receptor by the trichothecenes deoxynivalenol and satratoxin G. Toxicology 186, 51-65.

Davoren, M., Herzog, E., Casey, A., Cottineau, B., Chambers, G., Byrne, H.J., Lyng, F.M. 2007. In vitro toxicity evaluation of single walled carbon nanotubes on human A549 lung cells. Toxicol In Vitro 21,438-48.

Davoren. M., Ní Shúilleabháin, S., Hartl, M.G., Sheehan, D., O'Brien, N.M., O'Halloran. J., Van Pelt, F.N., Mothersill. C. 2005. Assessing the potential of fish cell lines as tools for the cytotoxicity testing of estuarine sediment aqueous elutriates. Toxicol In Vitro 19, 421-31.

Dendritech, Inc. http://www.dendritech.com/pamam.html

De Jong W.H. NanoImpactNet workshop on Protocols for assessment of biological hazards of engineered nanoparticles, Lausanne, March 2009.

Dobrovolskaia, M.A., Aggarwal, P., Hall, JB., McNeil, S.E. 2008. Preclinical study to understand nanoparticle interaction with the immuno system and its potential effects on nanoparticle biodistribution. Mol. Pharm. 5, 487-495.

Donaldson, K., Tran, L., Jimenez, L.A., Duffin, R., Newby, D.E., Mills, N., MacNee, W., Stone, V. 2005. Combustion-derived nanoparticles: a review of their toxicology following inhalation exposure. Part Fibre Toxicol. 2, 10.

Donaldson, K., Aitken, R., Tran, L., Stone, V., Duffin, R., Forrest, G., Alexaner, A. 2006. Carbon nanotubes: a review of their properties in relation to pulmonary toxicology and work place safety. Toxicol. Sci. 92, 5-22.

Driscoll K.E. 2000. TNF-α and MIP-2: role in particle induced inflammation and regulation by oxidative stress. Toxicol Lett. 112-113, 177-184.

Driscoll, K.E., Hassenbein, D.G., Howard, B.W., Isfort, R.J., Cody, D., Tindal, M.H., Carter, J.M. 1995. Cloning, expression, and functional characterization of rat macrophage inflammatory protein 2: a neutrophil chemoattractant and epithelial cell mitogen. J. Leuk. Biol. 58, 359–364.

Duncan, R., Izzo, L. 2005. Dendrimer biocompatibility and toxicity. Adv. Drug Delivery Rev. 57, 2215–2237

Emanuele, A. D., Attwood, D. 2005. Dendrimer-drug interactions. Adv. Drug Delivery Rev. 57, 2147–2162.

Elbekai, R.H and El-Kadi, A.O.S., 2005. The role of oxidative stress in the modulation of aryl hydrocarbon receptor-regulated genes by $As^{3+,}$ $Cd^{2+,}$ and $Cr^{6+.}$ Free RadicalBiol. Med. 39, 1499–1511.

Gillies, E.R., Frechet, J.M.J. 2005. Dendrimers and dendritic polymers in drug delivery. Drug Discovery Today 10, 35-43.

Herzog, E., Byrne, H.J., Casey, A., Davoren, M., Lenz, A-G., Maier, K.L., Duschl, A., Oostingh, G.J. 2009. SWCNT suppress inflammatory mediator responses in human lung epithelium in vitro. Toxicology and Applied Pharmacology 234, 378-390.

http://probes.invitrogen.com/media/pis/g002.pdf

Huang, R.Q., Qu, Y.H., Ke, W.L., Zhu, J.H., Pei, Y.Y., Jiang, C. 2007. Efficient gene delivery targeted to brain using a transferrin conjugated polyethylene glycol modified polyamidoamine dendrimer. FASEB J. 21, 1117-1125.

Hulikova, K., Benson, V., Svoboda, J., Sima, P., Fiserova, A. 2009. N-Acetyl-D-glucosamine-coated polyamidoamine dendrimer modulates antibody formation via natural killer cell activation. International Immunopharmacology 9, 792–799.

Kang, H., De-Long, R., Fisher, MH., Juliano, R.L. 2005. Tat-conjugated PAMAM Dendrimers as delivery agents for antisense and siRNA oligonucleotides. Pharmaceutical research 22, 2099-2106.

Kuo, J.H., Jan, M.S., Lin, Y.L. 2007. Interactions between U-937 human macrophages and poly(propyleneimine) dendrimers. J. Control Release. 120, 51-9.

Kukowska-Latallo, J.F., Candido, K.A., Cao, Z., Nigavekar, S.S., Majoros, I.J., Thomas, T.P., Balogh, L.P., Khan, M.K., Baker, J.R. 2005. Nanoparticle targeting of anticancer drug improves therapeutic response in animal model of human epithelial cancer. Cancer Res. 65, 5317-24.

Lanone, S., Boczkowski, J. 2006. Biomedical Applications and Potential Health Risks of Nanomaterials: Molecular Mechanisms. Curr Mol Med. 6, 651-63.

Lee, C.C., MacKay, J.A., Frechet, J.M.J., Szoka, F.C. 2005. Designing dendrimers for biological applications. Nat Biotechnol. 23, 1517–1526.

Lee, J.H., Cha, K.E., Kim, M.S., Hong, H.W., Chung, D.J., Ryu, G., Myung, H. 2009. Nanosized polyamidoamine (PAMAM) dendrimer-induced apoptosis mediated by mitochondrial dysfunction. Toxicol Lett. 190 , 202–207.

Li, N., Sioutas, C., Cho, A., Schmitz, D., Misra, C., Sempf, J., Wang, M, Oberley, T., Froines, J., Nel, A. 2003. Ultrafine particulate pollutants induce oxidative stress and mitochondrial damage. Environ Health Perspect. 111, 455-60.

Li, N., Xia, T., Nel, A.E. 2008. The role of oxidative stress in ambient particulate Matter-induced lung diseases and its implications in the toxicity of engineered nanoparticles. Free Radical Biol. Med. 44, 1689–1699.

Lubos, E., Handy, D.E., Loscalzo, J. 2008. Role of oxidative stress and nitric oxide in atherothrombosis. Front. Biosci. 13, 5323–5344.

Lynch, I., Cedervall, T., Lundqvist, M., Cabaleiro-Lago, C., Linse, S., Dawson, K. 2007. A. The nanoparticle-protein complex as a biological entity; A complex fluids and surface science challenge for the 21st century. Adv. Colloid Interface Sci. 13, 4–135.

Maeda, H., Matsumura, Y. 1986. A new concept on macromolecular therapeutics in cancer chemotherapy: mechanism of tumouritropic accumulation of proteins and the antitumour agents SMANCS. Cancer Res. 46, 6387-6392.

Monteiller, C., Tran, L., MacNee, W., Faux, S., Jones, A., Miller, B., Donaldson, K. 2007. The proinflammatory effect of low toxicity low solubulity particles, nanoparticles and fine particles on epithelial cell in vitro: the role of surface area. Occup. Environ. Med. 64, 609-615.

Mukherjee, S.P., Davoren, M., Byrne, H.J. 2009. In vitro mammalian cytotoxicological study of PAMAM dendrimers - Towards quantitative structure activity relationships Toxicol In Vitro, (In press).

Naha, P.C., Davoren, M., Casey, A., Byrne, H.J. 2009. An ecotoxicological study of poly(amidoamine dendrimers-towards quantitative structure activity relationship. Environ. Sci. Technol. 43, 6864-6869.

Nel, A., Xia, T., Madler, L., Ning, L. 2006. Toxic potential of materials at nanolevel. Science 311, 622-627.

Obedoster, G., Obedoster, E., Obedoster. A. 2005. Nanotoxicology: an emerging discipline evolving from studies of ultrafine particles. Environ. Health Perspect. 113, 823-839.

Organisation for Economic Co-operation and Development, 2001, Guideline (423) for Testing of Chemicals : Acute Oral Toxicity – Acute Toxic Class Method (http://www.oecd.org/dataoecd/17/50/1948370.pdf)

Park, E.J., Park, K. 2009. Oxidative stress and pro-inflammatory response induced by silica nanoparticles in vitro and in vivo. Toxicology Letters 184, 18-25.

Ragnvaldsson, D., Berglind, R., Tysklind, M., and Leffler, P. 2007. Environmental Hazard Screening of a Metal-polluted Site Using Pressurized Liquid Extraction and Two In Vitro Bioassays. A Journal of the Human Environment 36,494-501.

Rahman, I. 2000. Regulation of nuclear factor-κB, activator protein-1, and glutathione levels by tumor necrosis factor-α and dexamethasone in alveolar epithelial cells, Biochem. Pharmacol. 60, 1041–1049.

Rajananthanan, P., Attard, G. S., Sheikh, N. A., Morrow, W. J. 1999. Evaluation of novel aggregate structures as adjuvants: composition, toxicity studies and humoral responses. Vaccine 17, 715–730.

Sheng, K. C., Kalkanidis, M., Pouniotis, D.S., Esparon, S., Tang, C.K., Apostolopoulos, V., Geoffrey, A., Pietersz, G.A. 2008. Delivery of antigen using a novel mannosylated dendrimer potentiates immunogenicity in vitro and in vivo Eur. J. Immunol. 38, 424–436.

Stone, V., Johnston, H., Clift, M.J. 2007. Air pollution, ultrafine and nanoparticles toxicology: cellular and molecular interactions. IEEE Trans. Nanobiosci. 6, 331–340.

Svenson, S., Tomalia, D. A. 2005. Dendrimers in biomedical applications-reflections on the field. Adv. Drug Delivery Rev. 57, 2106–2129.

Venuganti, V. V. K., Perumal, O. P. 2008. Effect of Poly(amidoamine) (PAMAM) dendrimer on skin permeation of 5-fluorouracil. Int. J. Pharm. 361, 230–238.

Walley, K.R., Lukacs, N.W., Standiford, T.J., Strieter, R.M., Kunkel, S.L. 1997. Elevated levels of macrophage inflammatory protein 2 in severe murine peritonitis increase neutrophil recruitment and mortality. Infect. Immun. 65, 3847-3851.

Wang, W., Xiong, W., Wan, J., Sun, X., Xu, H., Yang, X. 2009. The decrease of PAMAM dendrimer-induced cytotoxicity by PEGylation via attenuation of oxidative stress. Nanotechnology, 11;20(10):105103.

Xia, T., Kovochich, M., Liong M., Zink J.I., Nel, A. E. 2008. Cationic Polystyrene Nanosphere Toxicity Depends on Cell-Specific Endocytic and Mitochondrial Injury Pathways. ACS Nano, 2, 85-96.

Xia, T., Kovochich, M., Brant, J., Hotze, M., Sempf, J., Oberley, T., Sioutas, C., Yeh, J. I., Wiesner, M. R., Nel, A. E. 2006. Comparison of the Abilities of Ambient and Manufactured Nanoparticles to Induce Cellular Toxicity According to an Oxidative Stress Paradigm. Nano Lett. 6, 1794–1807.

Yoo, H., Juliano, R.L. 2000. Enhanced delivery of antisense oligonucleotides with fluorophore-conjugated PAMAM dendrimers. Nucleic acid Research. 28, 4225-4231.

Legends of Tables

Table 1. EC_{50} data of PAMAM dendrimer G-4, G-5 and G-6 in Alamar blue (AB) and MTT assay for 24 hour exposure in J774A.1 cells.

Table 2. Zeta potential of PAMAM dendrimers in different media.

Legends of Figures

Figure 1. Comparison of cytotoxicity assay between AB and MTT of (a) G-4, (b) G-5 and (c) G-6 PAMAM dendrimers in J774A.1 cells after 24h exposure. The data shown in mean ± SD (n=3).

Figure 2. (a) Time and generation dependence of toxic response of PAMAM dendrimers (G-4, G-5, G-6). (b) Correlation between number of surface amino group and the toxic response of PAMAM dendrimers at 24h exposure (AB assay). All the data are expressed in mean ± SD (n=3).

Figure 3. Confocal fluorescence and phase contrast micrographs of intracellular ROS generation following exposure to (a) negative control, (b) positive control (H_2O_2), (c) PAMAM G-4, (d) PAMAM G-5 and (e) PAMAM G-6. The data are shown after 2h exposure of PAMAM dendrimers.

Figure 4. (a) generation dependent intracellular reactive oxygen species (ROS) production following exposure to PAMAM dendrimers (G-4, G-5 and G-6) in J774A.1 cells at an exposure concentration of 1μM. The data are presented in mean ± SD (n=3), (b) correlation between the production of intracellular ROS and number of surface primary amino groups.

The data is presented upon the exposure of different concentration of PAMAM dendrimers with mean ± SD.

Figure 5. The level of MIP-2 secreted after exposure of J774A.1 cells to (a)G-4, (b) G-5 and (c) G-6 PAMAM dendrimers for 6h, 12h, 24h, 48h and 72h. These data are presented in mean ± SD (n=3).

Figure 6. Generation dependent MIP-2, IL-6 and TNF-α secretion after 24h exposure of PAMAM dendrimers (G-4, G-5 and G-6) in J774A.1 cells. The data are shown as mean ± SD (n=3).

Figure 7. Correlation between inflammatory mediator (a) MIP-2, (b) IL-6 and (c) TNF-α response and the surface area of PAMAM dendrimers (G-4, G-5 and G-6). All the data are presented in mean ± SD (n=3).

Figure 8. (a) Schematic of the systematic sequence of events in J774A.1 cells following exposure to PAMAM dendrimers. (b) represents the schematic of different responses as a function of time.

Table 1.

Different media	PAMAM G-4 in mV	PAMAM G-5 in mV	PAMAM G-6 in mV
Milli-Q water	8.3 ± 5.5	21.5 ± 8.7	26.5 ± 4.7
DMEM	6.7 ± 3.7	18.0 ± 2.1	14.4 ± 3.0
5 % J774A.1 Cell culture media	-2.9 ± 1.1	-3.1 ± 0.9	-3.9 ± 0.4

Table 2.

PAMAM Dendrimer	**EC_{50} of AB assay in (μM)**	**EC_{50} of MTT assay in (μM)**
G-4	1.6 ± (0.3)	1.4 ± (0.3)
G-5	0.5 ± (0.2)	0.5 ± (0.2)
G-6	0.3 ± (0.1)	0.2 ± (0.1)

Figure 1. a.

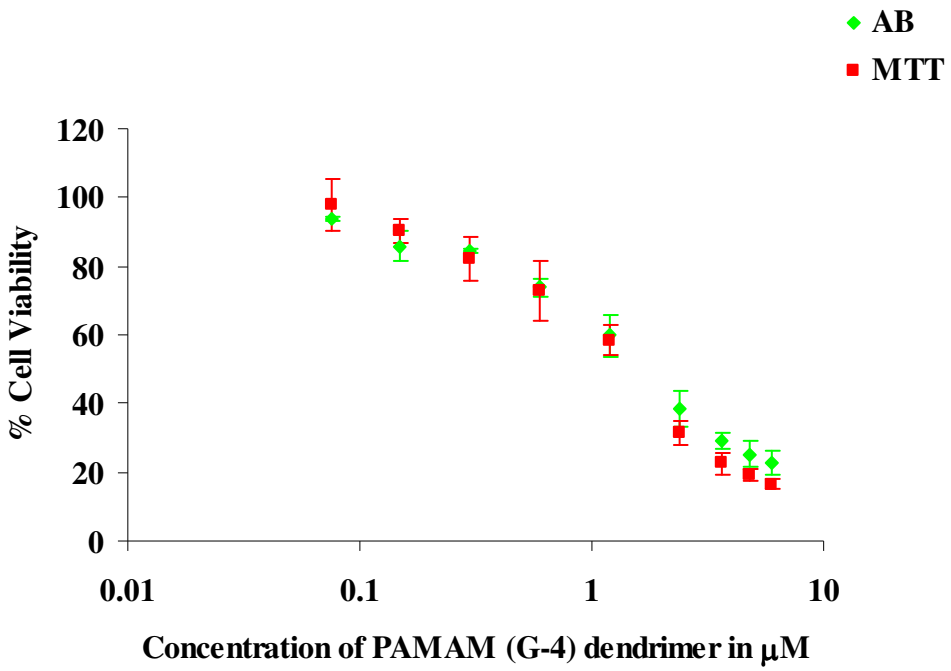
AB
MTT
120
100
80
60
40
20
0
% Cell Viability
0.01
0.1
1
10
Concentration of PAMAM (G-4) dendrimer in μM

b.

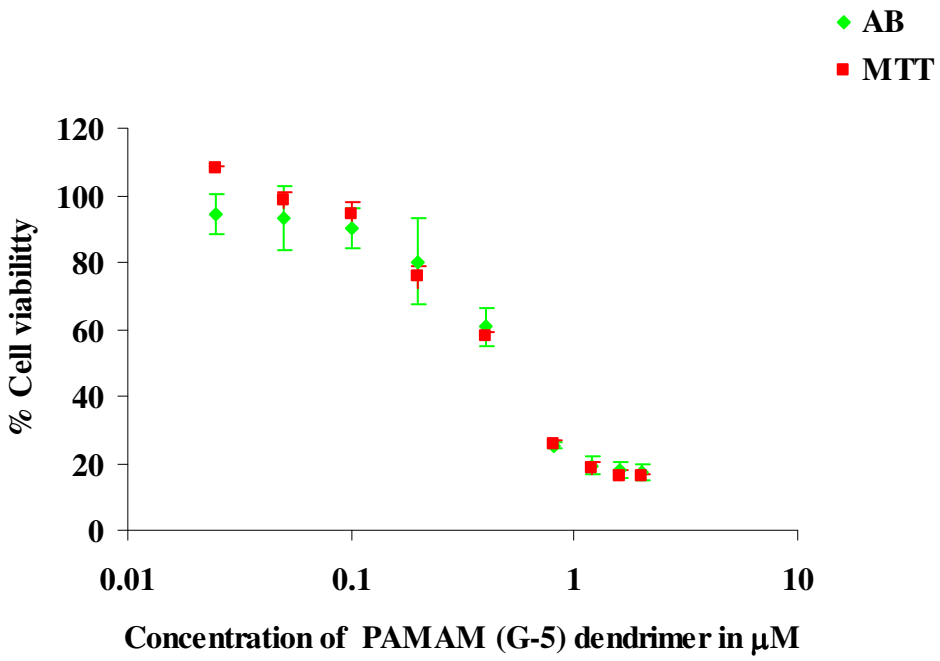
AB
MTT
120
100
80
60
40
20
0
% Cell viabilitty
0.01
0.1
1
10
Concentration of PAMAM (G-5) dendrimer in μM

c.

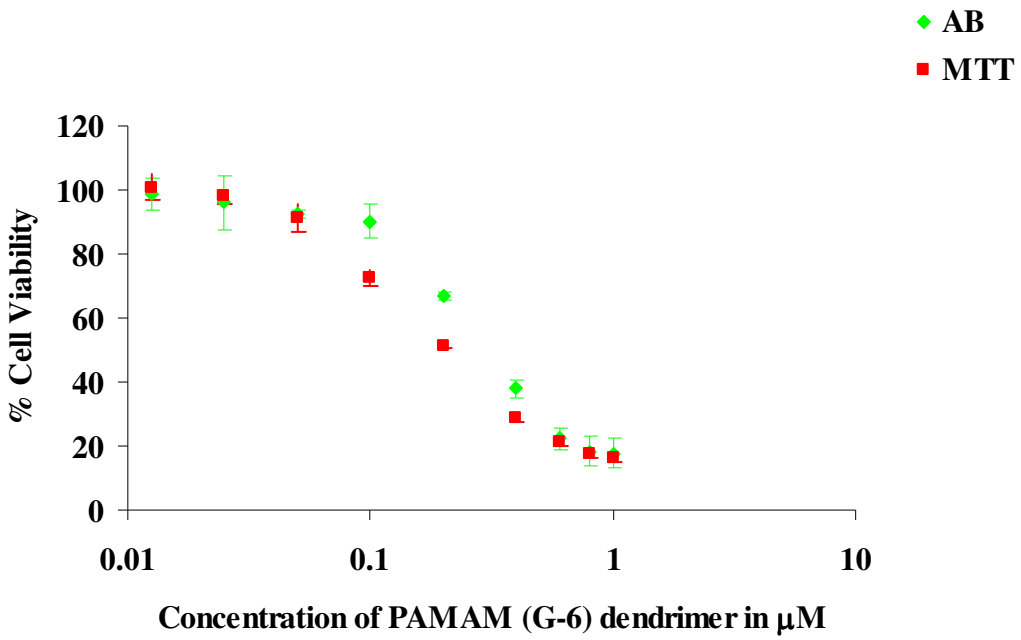
AB
MTT
120
100
80
60
40
20
0
% Cell Viability
0.01
0.1
1
10
Concentration of PAMAM (G-6) dendrimer in μM

Figure 2. a.

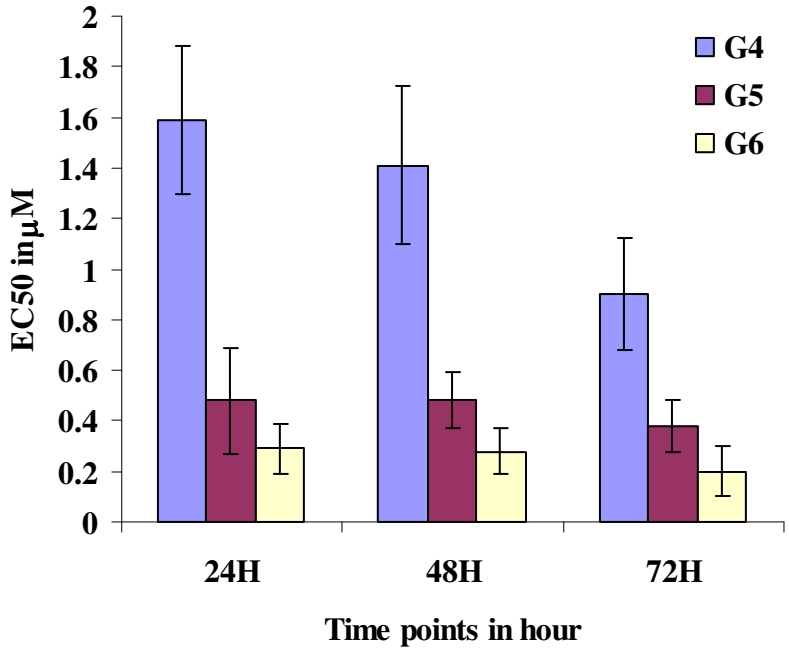
2
1.8
1.6
1.4
1.2
1
0.8
0.6
0.4
0.2
0
EC50 inμM
G4
G5
G6
24H
48H
72H
Time points in hour

b.

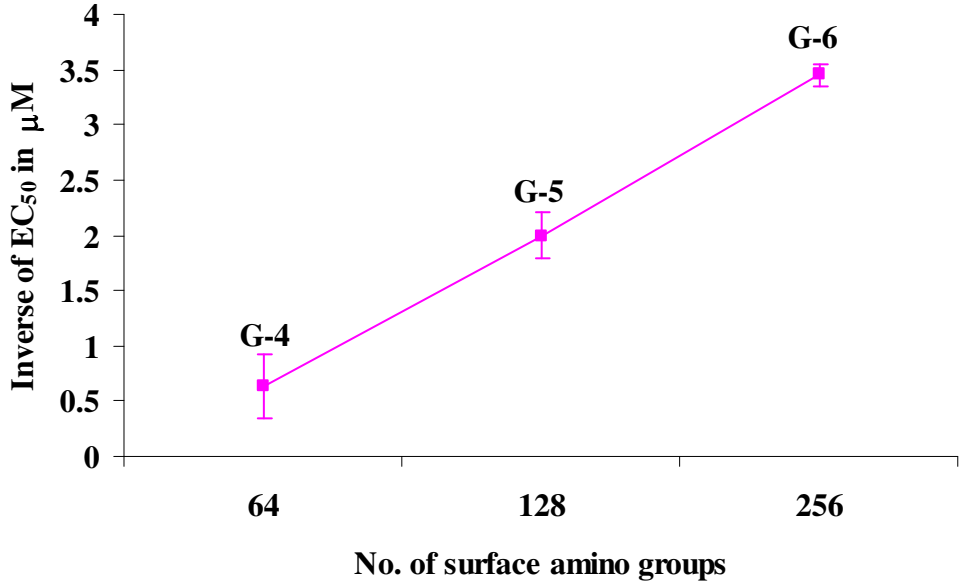
4
3.5
3
2.5
2
1.5
1
0.5
0
Inverse of EC50 in μM
G-4
G-5
G-6
64
128
256
No. of surface amino groups

Figure 3.

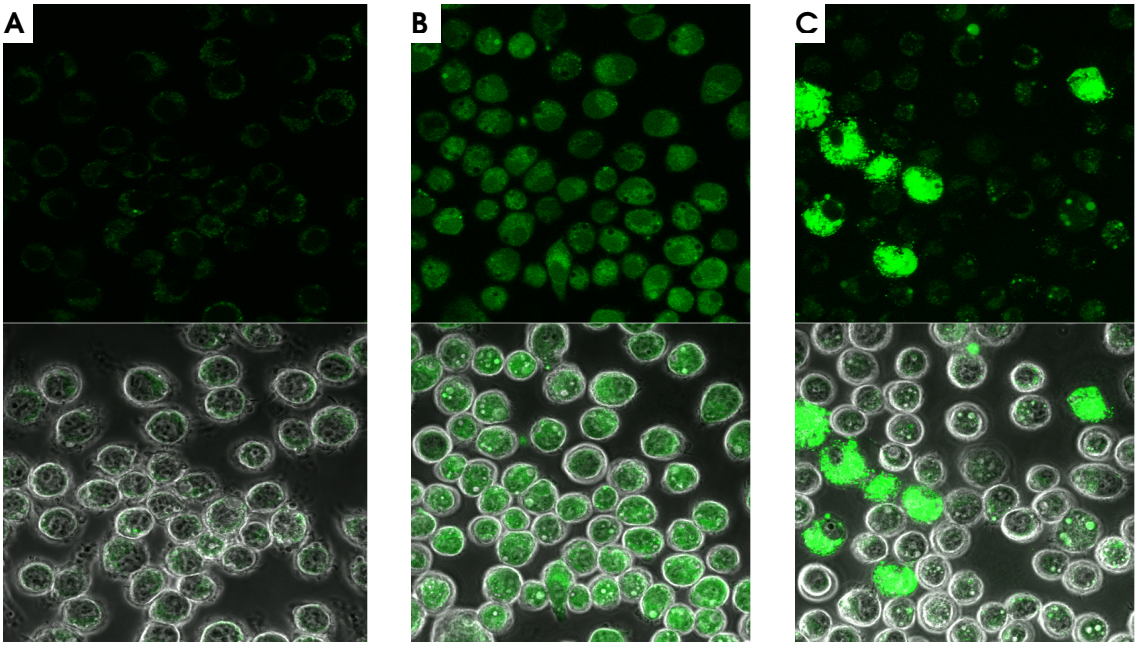

Figure 4a.

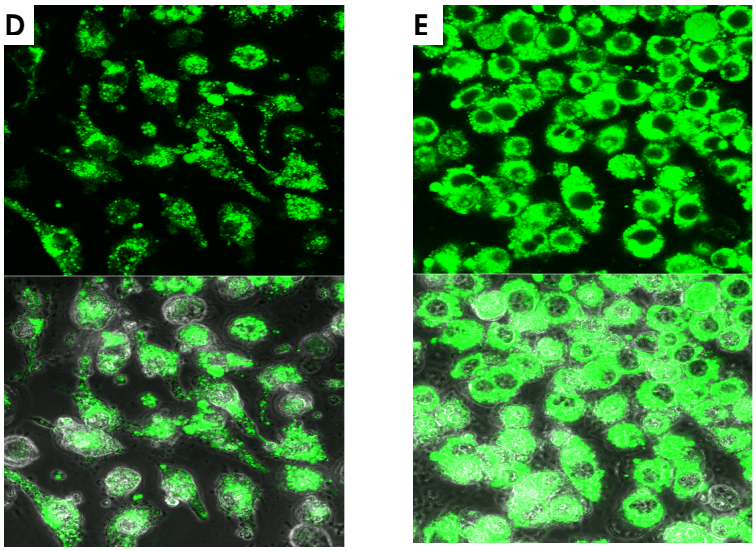

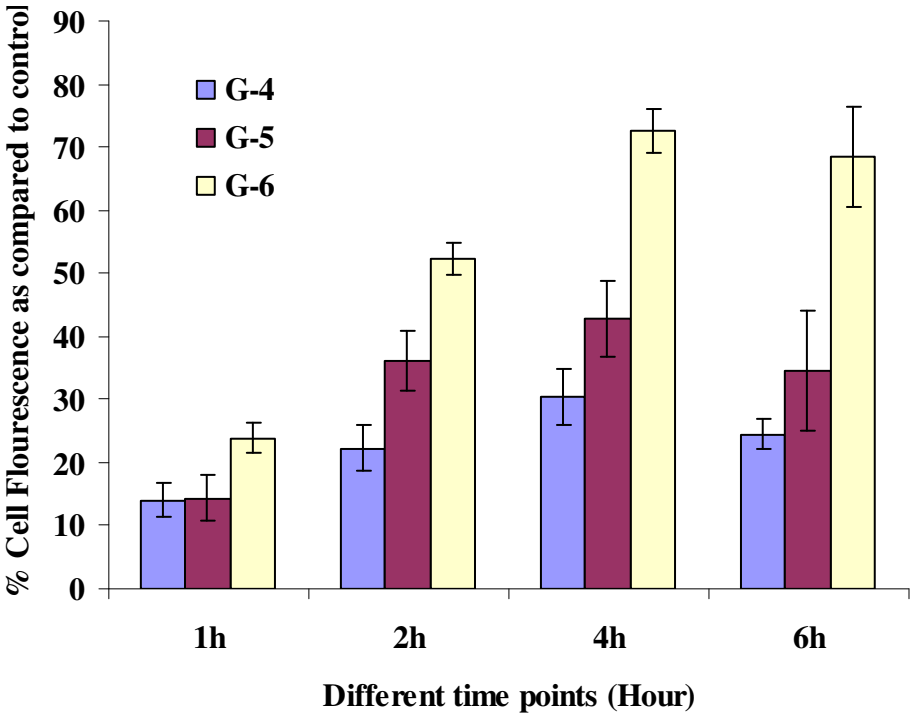
% Cell Flourescence as compared to control
90
80
70
60
50
40
30
20
10
0
G-4
G-5
G-6
1h
2h
4h
6h
Different time points (Hour)

Figure 4b.

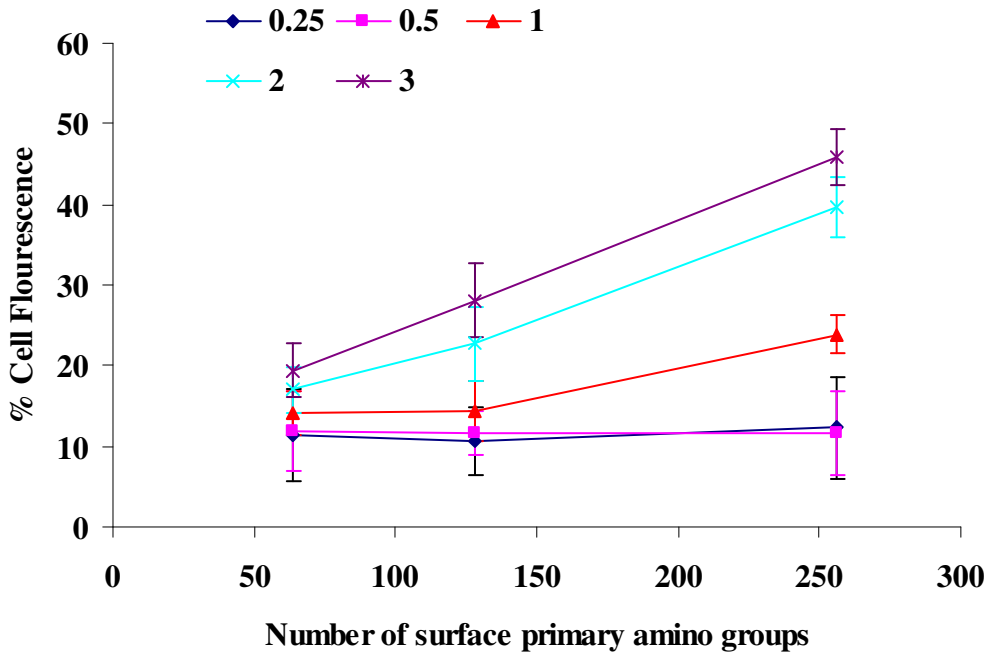
0.25
0.5
1
2
3
% Cell Flourescence
60
50
40
30
20
10
0
0
50
100
150
200
250
300
Number of surface primary amino groups

Figure 5. a.

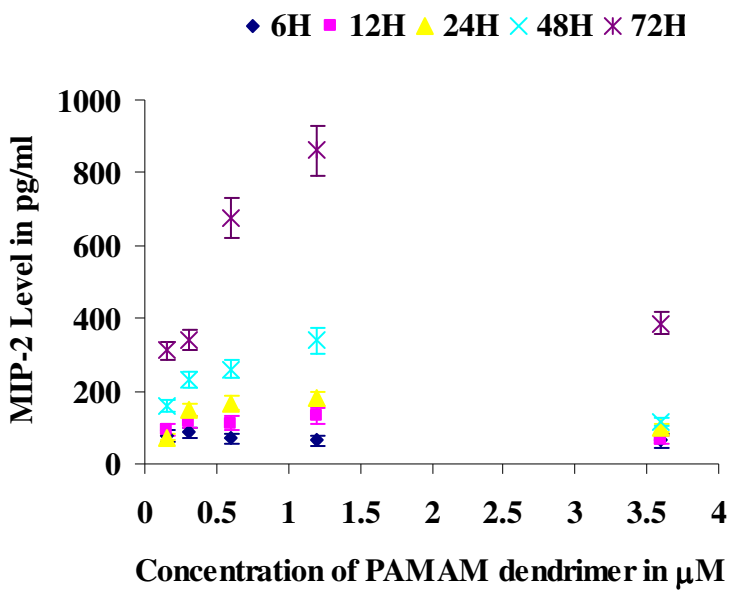
6H 12H 24H 48H 72H
MIP-2 Level in pg/ml
1000
800
600
400
200
0
0 0.5 1 1.5 2 2.5 3 3.5 4
Concentration of PAMAM dendrimer in µM

b.

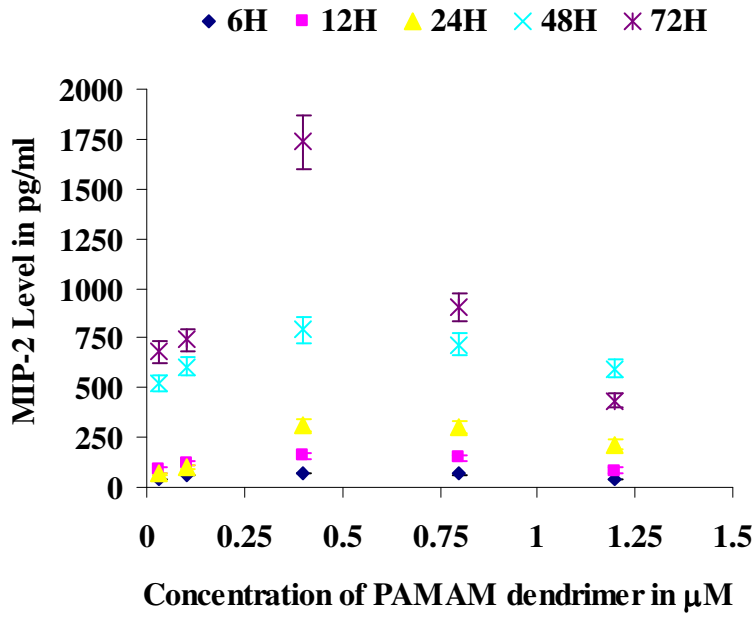
6H 12H 24H 48H 72H
MIP-2 Level in pg/ml
2000
1750
1500
1250
1000
750
500
250
0
0 0.25 0.5 0.75 1 1.25 1.5
Concentration of PAMAM dendrimer in µM

c.

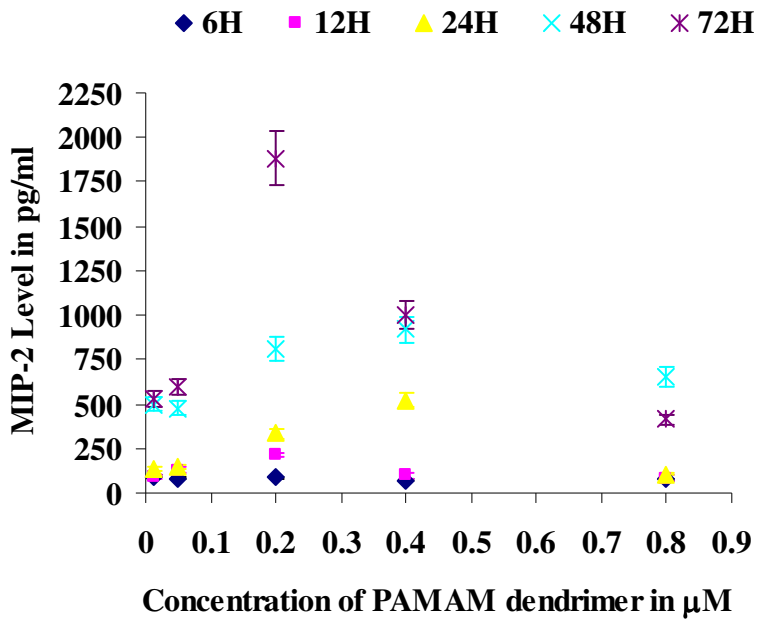
6H
12H
24H
48H
72H
MIP-2 Level in pg/ml
2250
2000
1750
1500
1250
1000
750
500
250
0
0
0.1
0.2
0.3
0.4
0.5
0.6
0.7
0.8
0.9
Concentration of PAMAM dendrimer in µM

Figure 6.

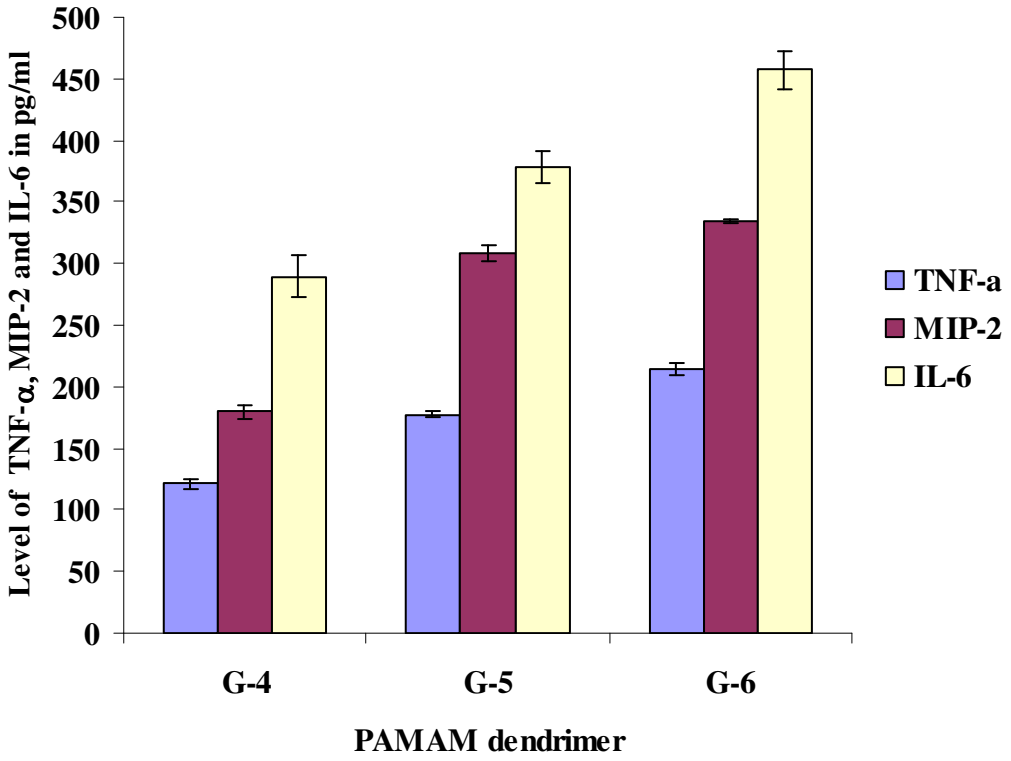
Level of TNF-α, MIP-2 and IL-6 in pg/ml
500
450
400
350
300
250
200
150
100
50
0
G-4
G-5
G-6
PAMAM dendrimer
TNF-a
MIP-2
IL-6

Figure 7. a.

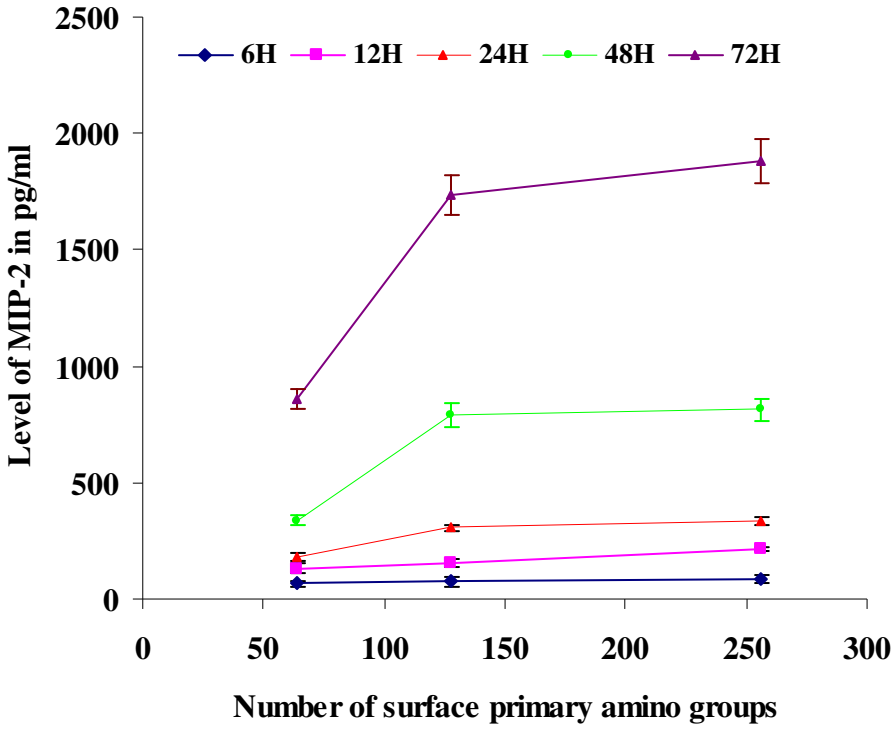
6H
12H
24H
48H
72H
Level of MIP-2 in pg/ml
2500
2000
1500
1000
500
0
0
50
100
150
200
250
300
Number of surface primary amino groups

b.

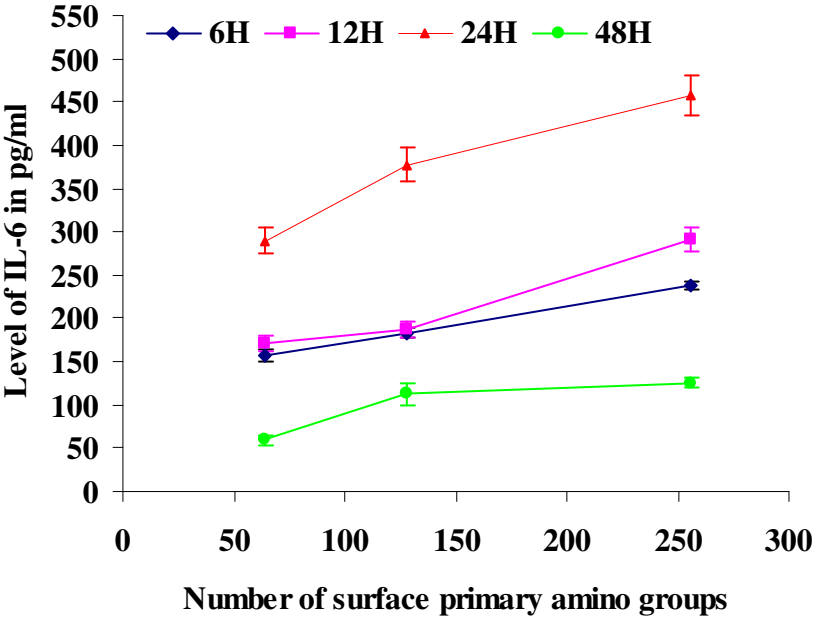
6H
12H
24H
48H
Level of IL-6 in pg/ml
550
500
450
400
350
300
250
200
150
100
50
0
0
50
100
150
200
250
300
Number of surface primary amino groups

c.

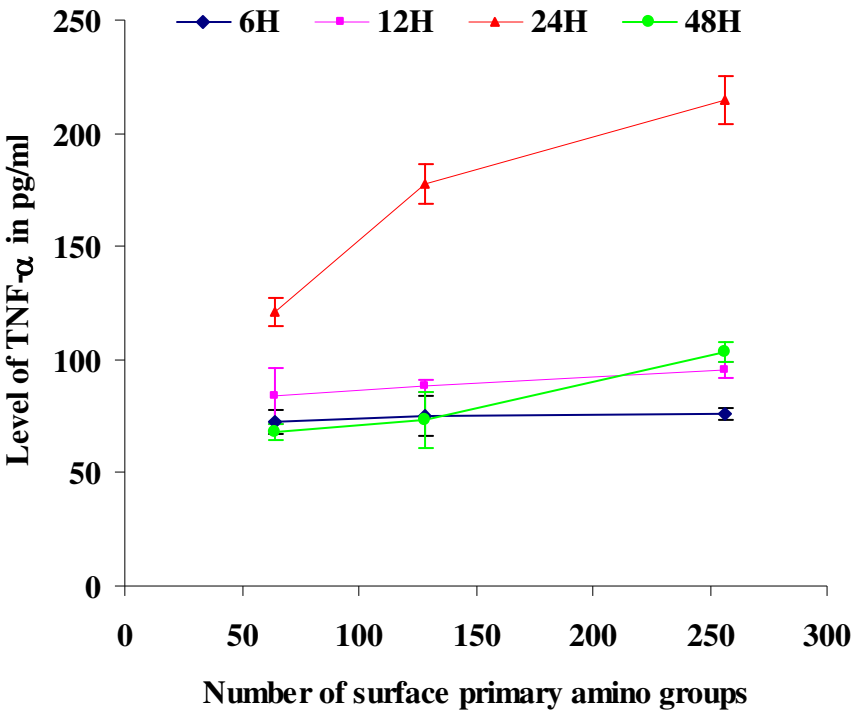
6H
12H
24H
48H
250
200
150
100
50
0
Level of TNF-α in pg/ml
0
50
100
150
200
250
300
Number of surface primary amino groups

Figure 8a.

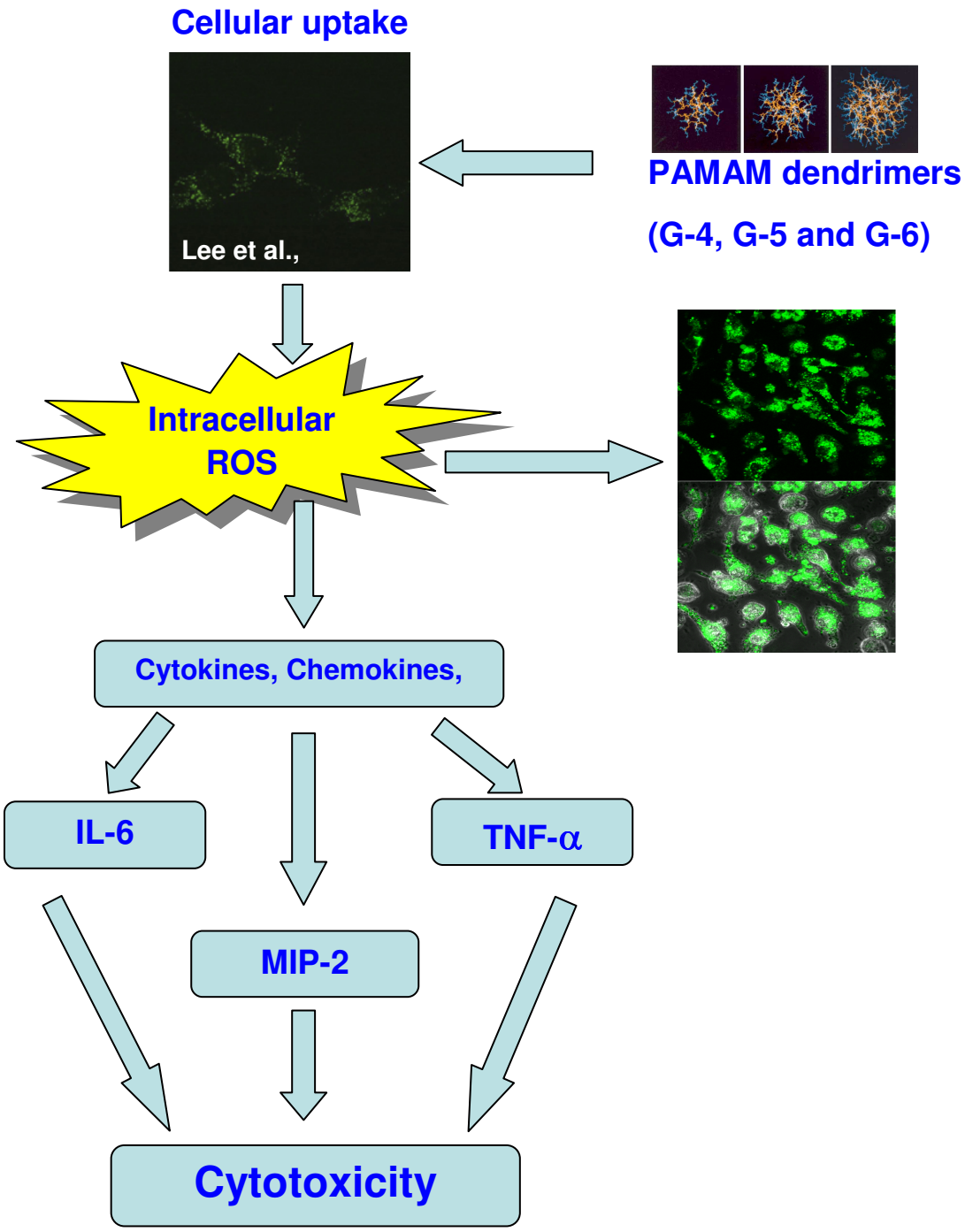
Cellular uptake
Lee et al.,
PAMAM dendrimers
(G-4, G-5 and G-6)
Intracellular
ROS
Cytokines, Chemokines,
IL-6
TNF-α
MIP-2
Cytotoxicity

b.

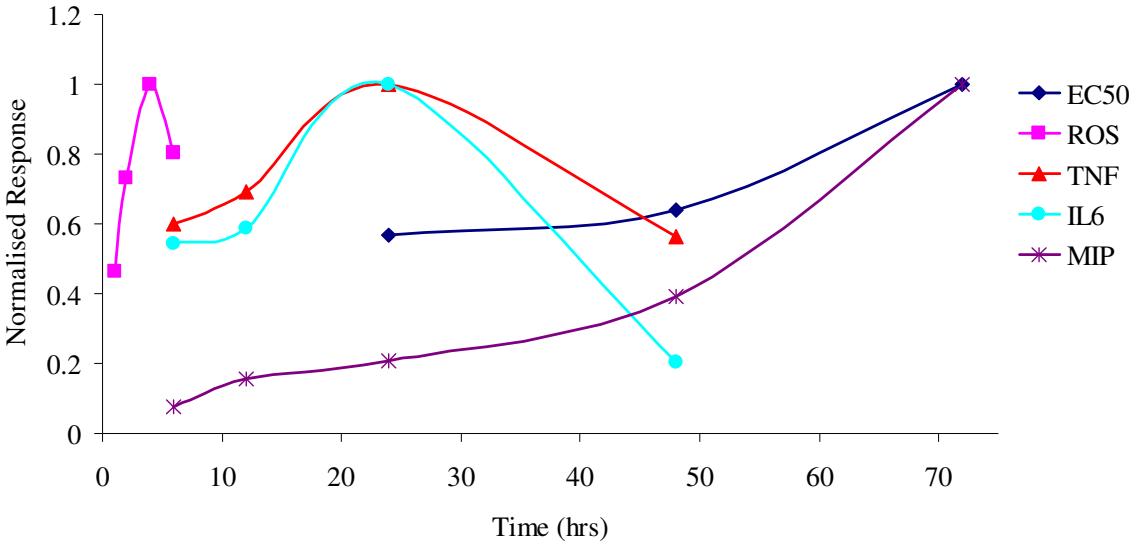
1.2
1
0.8
0.6
0.4
0.2
0
Normalised Response
0
10
20
30
40
50
60
70
Time (hrs)
EC50
ROS
TNF
IL6
MIP

Supporting information for

Reactive Oxygen Species Induced cytokines production and cytotoxicity of PAMAM dendrimers in J774A.1 cells

Pratap C. Naha[ab] Maria Davoren[a], Fiona M. Lyng[a] and Hugh J. Byrne[b]*

[a]Radiation and Environmental Science Centre, Focas Research Institute, Dublin Institute of Technology, Kevin Street, Dublin 8, Ireland.

[b]NanoLab, Focas Research Institute, Dublin Institute of Technology, Kevin Street, Dublin 8, Ireland.

***Corresponding Author**

Pratap C. Naha,

Radiation and environmental Science Centre

Focas Research Institute, Dublin Institute of Technology,

Kevin Street, Dublin 8, Ireland.

E mail address: pratap.naha@dit.ie

Ph: +353 1 4027956

Fax : +353 1 402 7901

Figure S.1.a.

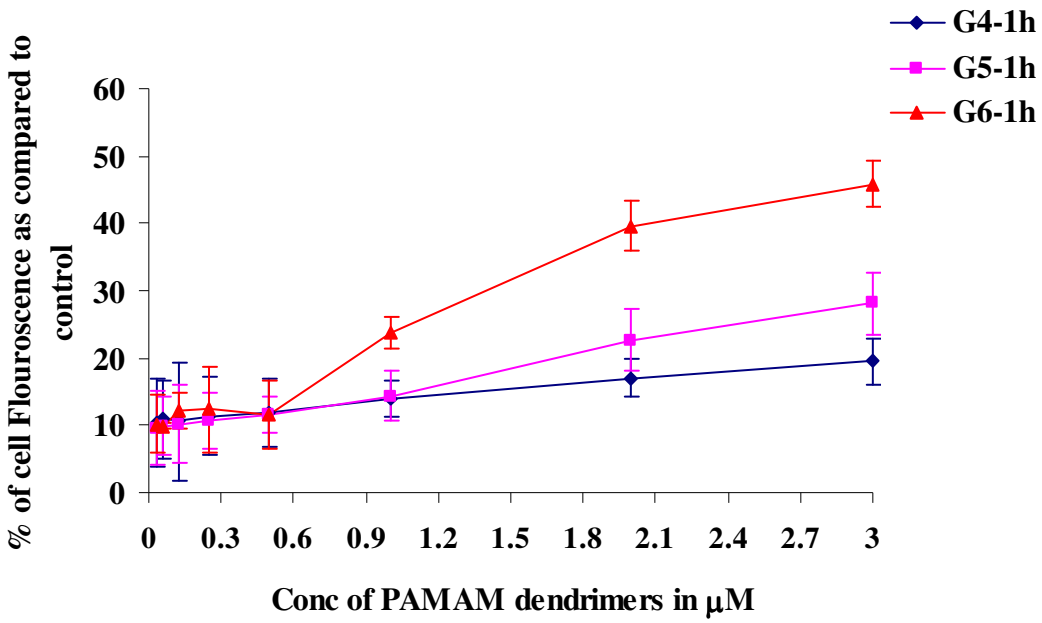
G4-1h
G5-1h
G6-1h
% of cell Flouroscence as compared to control
60
50
40
30
20
10
0
0
0.3
0.6
0.9
1.2
1.5
1.8
2.1
2.4
2.7
3
Conc of PAMAM dendrimers in µM

b.

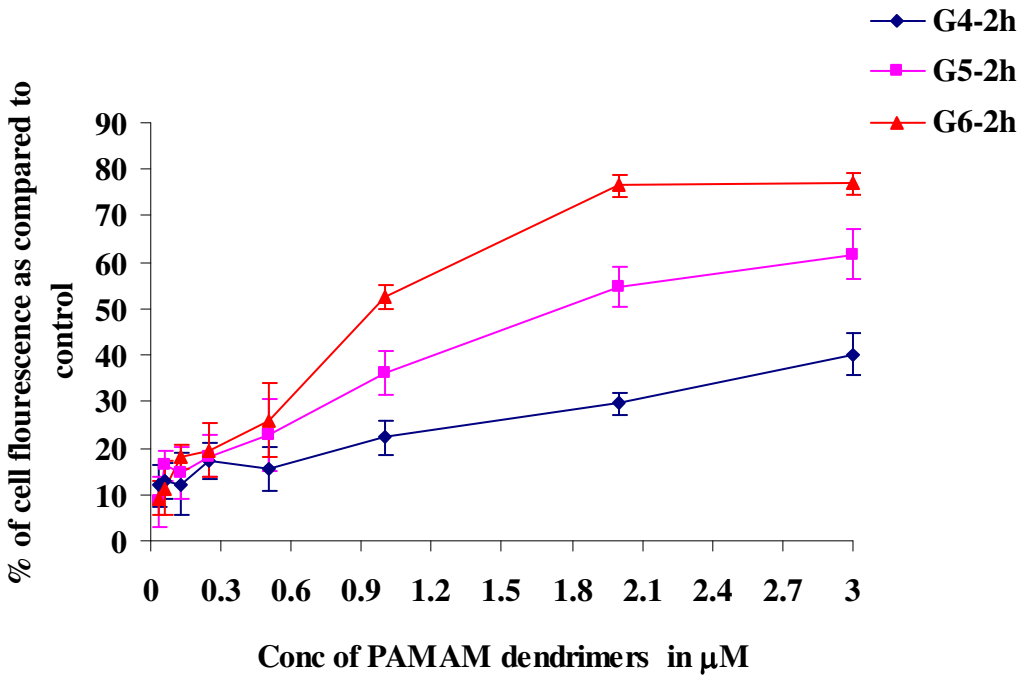
G4-2h
G5-2h
G6-2h
% of cell flourescence as compared to control
90
80
70
60
50
40
30
20
10
0
0
0.3
0.6
0.9
1.2
1.5
1.8
2.1
2.4
2.7
3
Conc of PAMAM dendrimers in µM

c.

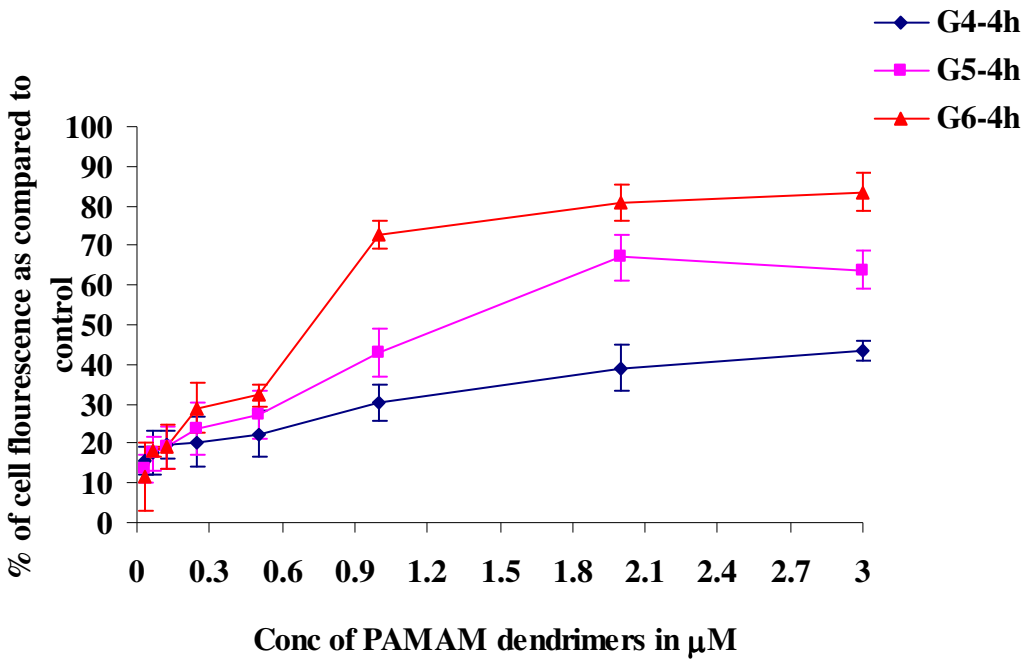

d.

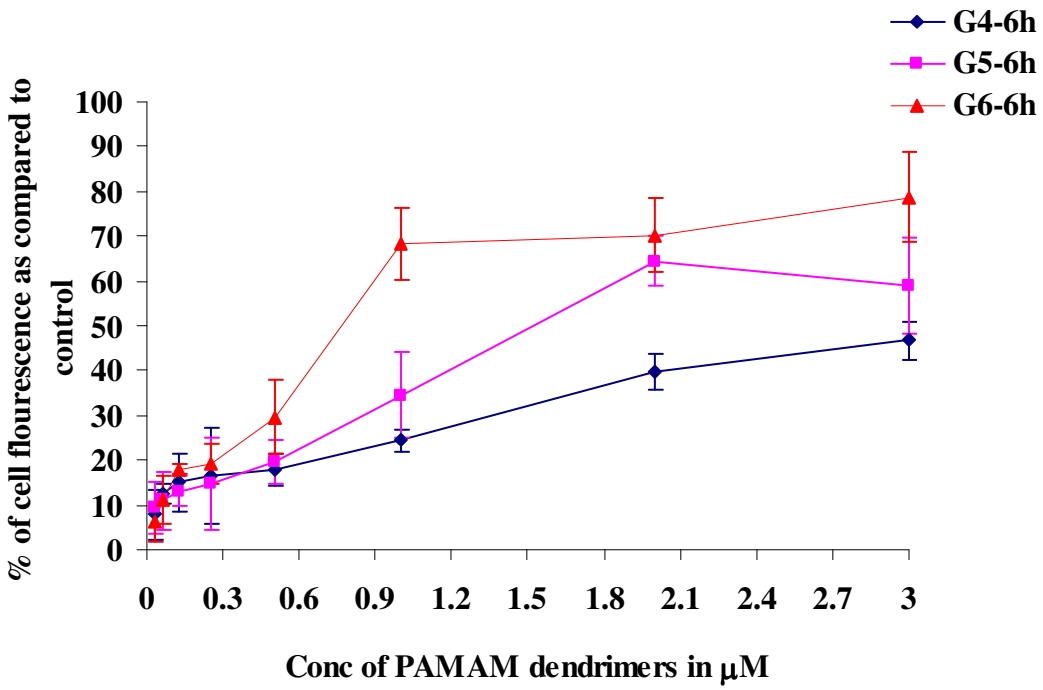

Figure S.2. a

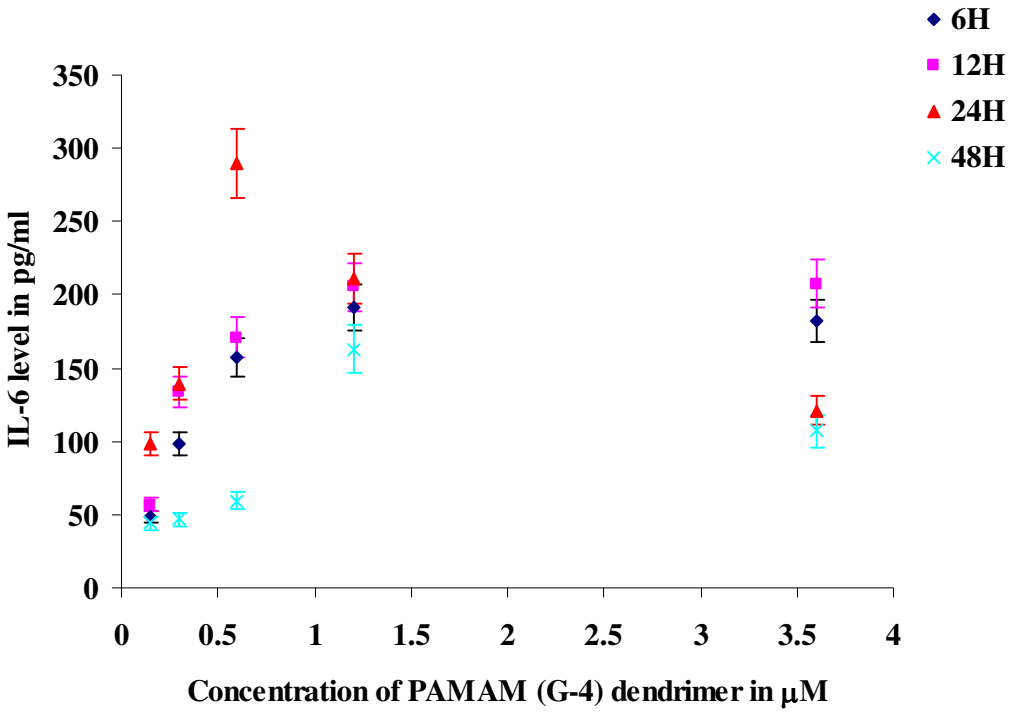
6H
12H
24H
48H
IL-6 level in pg/ml
350
300
250
200
150
100
50
0
0
0.5
1
1.5
2
2.5
3
3.5
4
Concentration of PAMAM (G-4) dendrimer in µM

b.

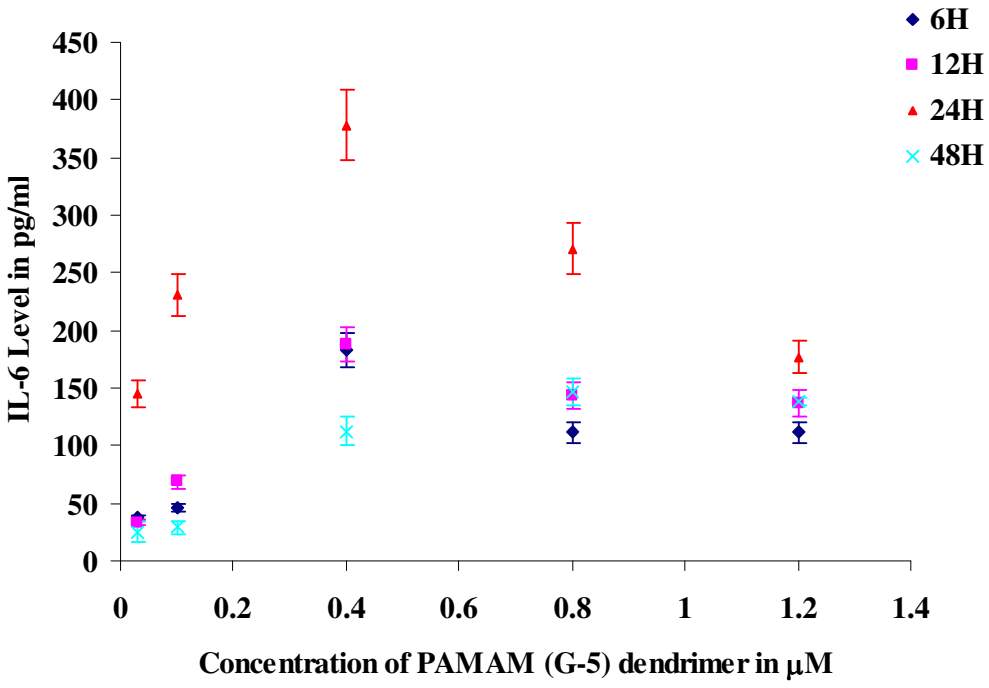
6H
12H
24H
48H
IL-6 Level in pg/ml
450
400
350
300
250
200
150
100
50
0
0
0.2
0.4
0.6
0.8
1
1.2
1.4
Concentration of PAMAM (G-5) dendrimer in µM

c.

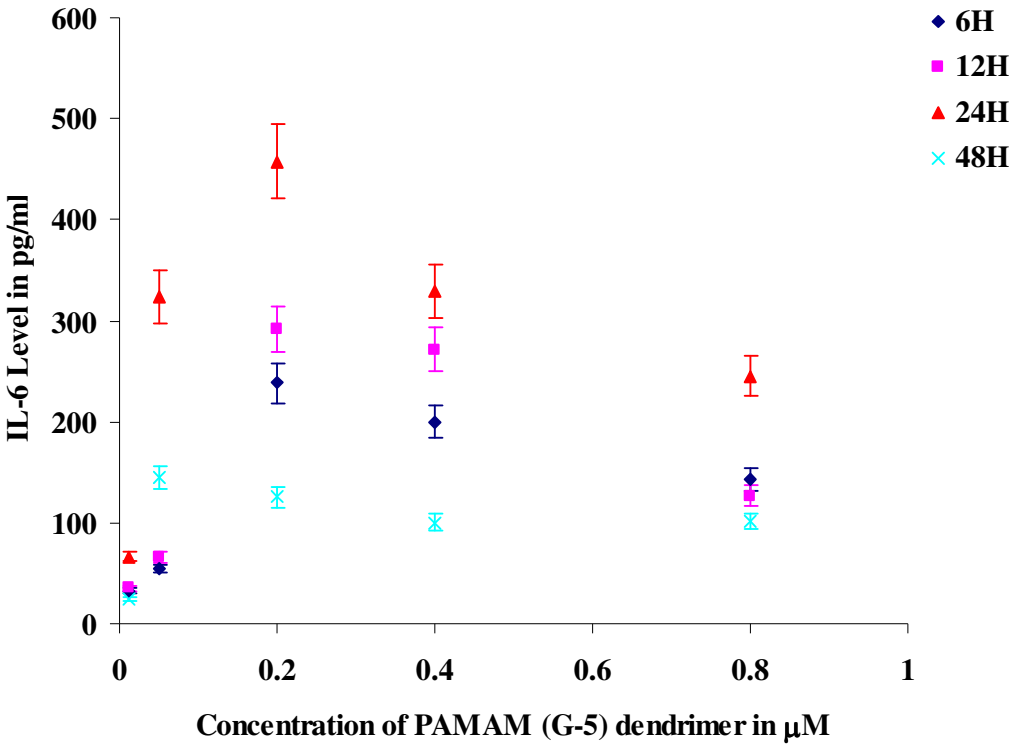
600
500
400
300
200
100
0
IL-6 Level in pg/ml
0
0.2
0.4
0.6
0.8
1
Concentration of PAMAM (G-5) dendrimer in μM
6H
12H
24H
48H

Figure S.3. a

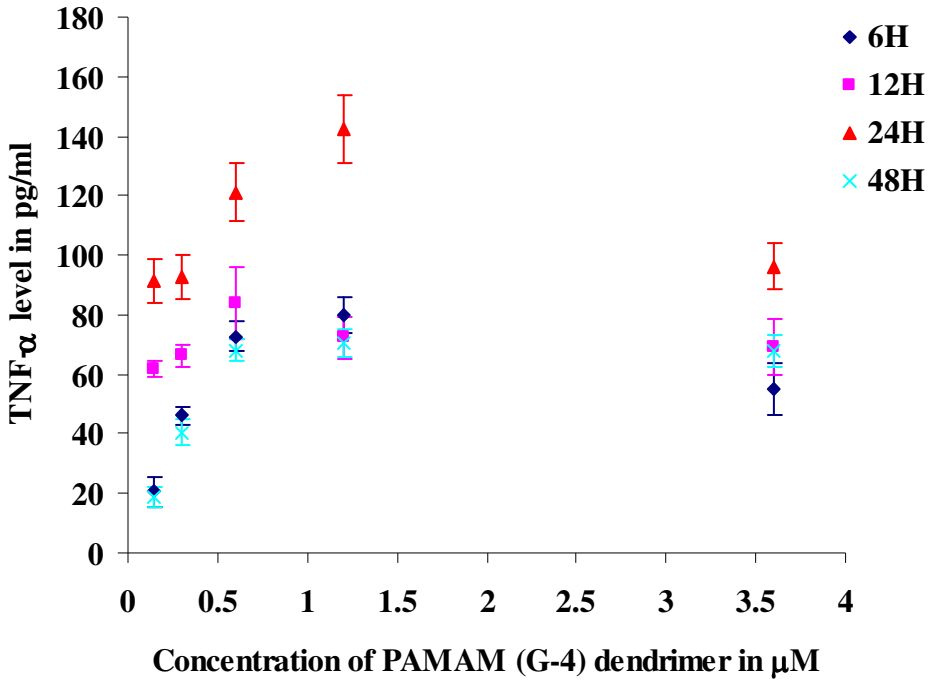
180
160
140
120
100
80
60
40
20
0
TNF-α level in pg/ml
0
0.5
1
1.5
2
2.5
3
3.5
4
Concentration of PAMAM (G-4) dendrimer in µM
6H
12H
24H
48H

b.

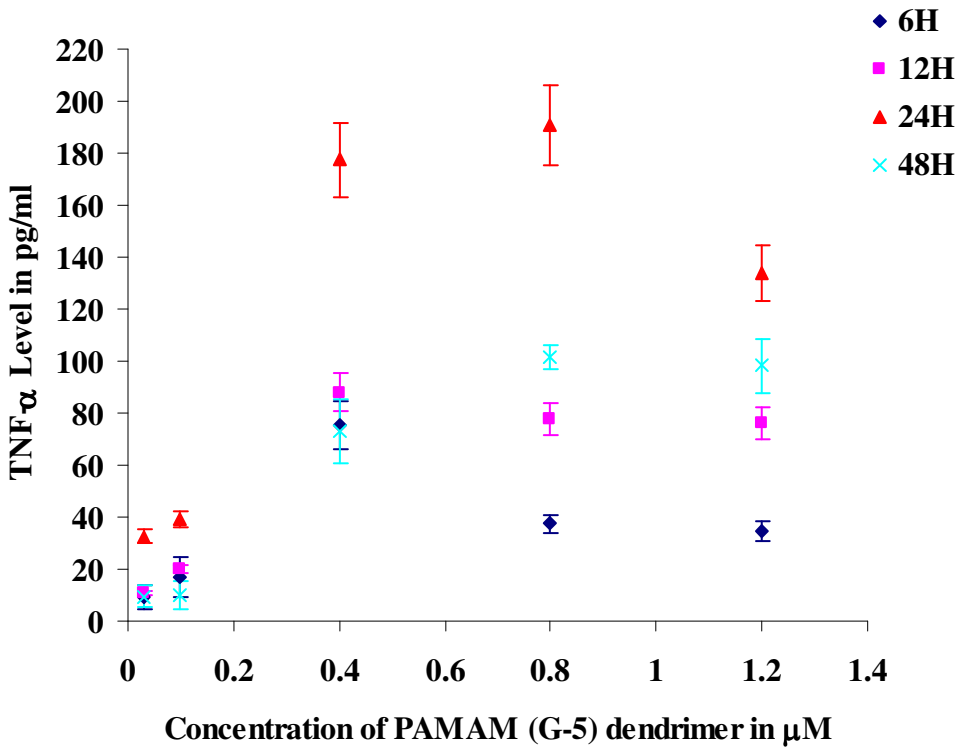
220
200
180
160
140
120
100
80
60
40
20
0
TNF-α Level in pg/ml
0
0.2
0.4
0.6
0.8
1
1.2
1.4
Concentration of PAMAM (G-5) dendrimer in µM
6H
12H
24H
48H

c.

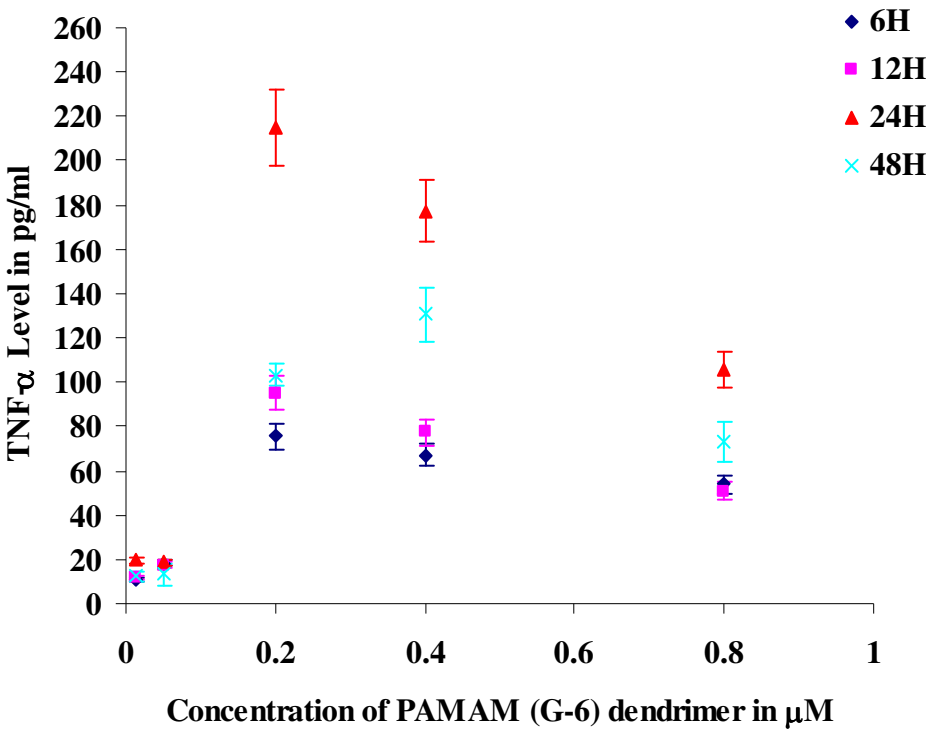
6H
12H
24H
48H
TNF-α Level in pg/ml
260
240
220
200
180
160
140
120
100
80
60
40
20
0
0
0.2
0.4
0.6
0.8
1
Concentration of PAMAM (G-6) dendrimer in μM

Legends of Figures

Figure S1. Concentration and time dependent intracellular ROS generation by G-4, G-5 and G-6 at (a) 1, (b) 2, (c) 4 and (d) 6 h exposure time points. The data are presented as mean ± SD (n=3).

Figure S2. Secretion of IL-6 following exposure of (a) G-4, (b) G-5 and (c) G-6 in J774A.1 cells at 6, 12, 24and 48 h time points. The data are presented as mean ± SD (n=3).

Figure S3. Secretion of TNF-α upon the exposure of (a) G-4, (b) G-5 and (c) G-6 in J774A.1 cells at 6, 12, 24 and 48 h time points. The data are presented as mean ± SD (n=3).